Periodic Event-triggered Fault Detection for Safe Platooning Control of Intelligent and Connected Vehicles

Lu Wang, Manjiang Hu, Yougang Bian, *Member, IEEE*, Ge Guo, *Senior Member, IEEE*, Shengbo Eben Li, *Senior Member, IEEE*, Boli Chen *Member, IEEE*, Zhihua Zhong

***Abstract*—Fault detection is not only a useful approach to guarantee the safety of a vehicle platooning system but also an indispensable part of functional safety for future connected automated vehicle development. This paper mainly concentrates on the network-based fault detection problem of a vehicle platoon with undirected topologies under a periodic event-triggered strategy (PETS). Firstly, we present a periodic event-triggered fault detection filter to generate a residual signal for this vehicle platoon subject to actuator faults and external disturbances, where PETS is employed to reduce bandwidth utilization and save communication resources. Secondly, by using the network-based fault detection filter, the vehicle platooning system, and a fault weighting system, a residual system is developed to formulate the design of the fault detection filter problem as an H_∞ problem. Thirdly, based on Lyapunov-Krasovskii functionals, sufficient conditions are established to ensure that the residual system fulfills asymptotic stability with H_∞ performance, together with a threshold is also designed for each vehicle to judge whether the fault happens or not. Finally, numerical examples and field experiments are conducted to verify our findings.**

***Index Terms*—Intelligent and connected vehicle (ICV), fault detection, network-based fault detection filter, periodic event-triggered strategy (PETS), vehicle platooning system.**

I. Introduction

As an efficient intelligent transportation system approach, a vehicle platooning system has attracted considerable attention because of its outstanding advantages, containing highway capacity, improved road safety, reduced fuel consumption, and traffic congestion relief [1]–[5]. Furthermore, the vehicle platooning system has seen continued interest in recent work on the study of range policies [6], string stability [7], dynamics heterogeneity [8], communication time delays [9], reinforcement learning [10], [11], etc.

It should be noticed that most aforementioned studies focus on a full reliability assumption, in other words, it is supposed that all the system components work under ideal circumstances without considering any inherent failures/faults. However, in practical circumstances, component fault and failure are inevitable in a vehicle platooning system, such as actuator stuck, float, loss of effectiveness, and polluted measurements. These issues can destroy the stability and even the safety of the vehicle platooning system [12], [13]. Over the past few decades, numerous scholars have devoted themselves to studying fault detection, and meaningful works have also been applied to a variety of systems including Takagi-Sugeno fuzzy systems [14], power systems [15], etc. Typically, a fault detection method is to develop a prescribed threshold and a residual evaluation function. Once the residual function exceeds the threshold, an alarm signal will be generated instantly [16]. In [17], the authors designed a dynamic observer-based robust controller and used the states of the observer to generate a residual signal for fault detection. Yang et al. [18] not only proposed a fault detection strategy to detect actuator faults but also designed a dynamic output feedback control strategy to decrease the effects of external disturbances. However, most of the existing studies on fault detection mainly discuss the single vehicle [19] or the unmanned surface vehicle [43]. As far as we know, the development of fault detection strategies for vehicle platoon control remains challenging.

With the deployment of vehicle platoons, limited communication resources have become one of the main restrictive factors for platooning applications [20]. However, most existing studies about vehicle platooning systems are time-triggered, that is, each vehicle in a platoon transmits information to its neighbors during each sampling period [21], [22], and many inevitable communication drawbacks (e.g., data packet loss and communication time delays) are directly related to excessive use of communication resources [23]. Obviously, these cause a great waste of communication resources and unnecessary bandwidth utilization, particularly when the transmitted or updated states do not change fast. To deal with this issue, we can consider an event-triggered strategy (ETS) to coordinate

This study was supported by Hunan Provincial NSF of China (2023JJ10008), NSF of China (52172384, 52002126), and Young Elite Scientists Sponsorship Program by CAST (2022QNRC001). *(Corresponding authors: Yougang Bian.)*

L. Wang, M. J. Hu, and Y. G. Bian are with the State Key Laboratory of Advanced Design and Manufacturing Technology for Vehicle, College of Mechanical and Vehicle Engineering, Hunan University, Changsha 410082, China; M. J. Hu and Y. G. Bian are also with Wuxi Intelligent Control Research Institute of Hunan University, Wuxi, 214115, China (e-mail: wanglu_aine@163.com; manjiang_h@hnu.edu.cn; byg10@foxmail.com).

G. Guo is with the State Key Laboratory of Synthetical Automation for Process Industries, Northeastern University, Shenyang 110819, China; G. Guo is also with the School of Control Engineering, Northeastern University at Qinhuangdao, Qinhuangdao 066004, China (e-mail: geguo@yeah.net).

S. E. Li and Z. H. Zhong are with the School of Vehicle and Mobility, Tsinghua University, Beijing 100084, China; Z. H. Zhong is also with the Chinese Academy of Engineering, Beijing 100088 China (e-mail: lishbo@tsinghua.edu.cn; zhong_zh_tsing@126.com).

B. Chen is with the Department of Electronic and Electrical Engineering, University College London, London WC1E 6BT, U.K. (e-mail: boli.chen@ucl.ac.uk).

resources among vehicles in a platoon, that is, only sampling and updating the state data when the vehicle state changes exceed a predefined threshold [24]. Over the past decade, the ETS has been widely applied in networked systems [25], multi-agent systems [26] and nonlinear systems [27]. Recently, it has also been employed in vehicle platoon control [23], [28], [29]. By exploiting the fully distributed event-triggered controller, Wu et al. [28] discussed the leader-follower consensus of vehicle platoons with intermittent communication. In [29], the authors studied the design of platoon control and event-triggered communication strategies for vehicles with limited communication resources. However, a key point when designing an ETS is that a lower bound of inter-event times must be given, which implies the defined threshold needs to avoid Zeno behavior. Regrettably, achieving this requirement may not be easy. Given this, a periodic ETS (PETS) has been proposed, where measurements of states and computations of the thresholds and the residuals are only at periodic time instants rather than continuously in time. In [30], the PETS for linear systems was proposed, and then the authors [31] extended it to nonlinear networked systems. Note that limited research has focused on the control of the vehicle platoon [32]. As we are aware, PETS-based fault detection in the vehicle platooning system is still a topic that has not been discussed yet. Therefore, this study proposes a network-based fault detection filter with the PETS to improve the safety of vehicle platooning systems.

Inspired by the discussions mentioned above, our works aim to investigate PETS-based fault detection for a vehicle platoon with undirected topologies in a network environment subject to actuator faults and external disturbances (see Fig. 1). The main contributions are as follows.

1) This study proposes a novel approach for detecting the actuator faults of a vehicle platooning system under external disturbances, designing a network-based fault detection filter. To save more communication resources and reduce unnecessary bandwidth utilization effectively, a PETS is applied in the design of this fault detection filter.

2) To acquire a better fault detection performance, we design a fault weighting system, and by combining with the vehicle platoon, the network-based fault detection filter, and the fault weighting system, a residual system is constructed to guarantee fault detection filter design.

3) By choosing a suitable Lyapunov-Krasovskii functional and inequality techniques, we develop several theorems to ensure asymptotic stability with H_∞ performance of the residual system and obtain fault detection filter's parameters. In addition, we also formulate a threshold for each following vehicle to judge whether a fault happens or not.

The rest of this paper is summarized as follows. In Section II, we introduce some preliminaries about vehicle platoon modeling. In Sections III and IV, we propose the design of the fault detection filter with the PETS and establish several theorems for a residual system, respectively. In Section V, numerical experiments and field experiments are presented to verify the validity of acquired results. Section VI draws the conclusions.

Notations: $\Lambda_2[0,+\infty)$ stands for the linear space of square-integrable vectors over the time interval $[0,+\infty)$. $[M]_s$ denotes a simplified notation of $M+M^T$. Let $\mathbb{R}^n$ be the n-dimensional Euclidean space and $\mathbb{R}^{n\times m}$ be the space of $n\times m$ real matrices. The symmetric elements of the symmetric matrix will be defined by $\{*\}$. The space of functions $\varrho:[\sigma_1,\sigma_2]\to\mathbb{R}^n$ that have a finite $\lim_{z\to\sigma_2^-}\varrho(z)$, are absolutely continuous on $[\sigma_1,\sigma_2)$, and have square integrable first-order derivatives is defined by $\mathcal{Y}[\sigma_1,\sigma_2)$ and $\|\varrho\|_{\mathcal{Y}}=\max_{z\in[\sigma_1,\sigma_2]}|\varrho(z)|+[\int_{\sigma_1}^{\sigma_2}|\dot{\varrho}(z)|^2dz]^{\frac{1}{2}}$. $0_{mN\times nN}=0\times(I_N\otimes Q)\in\mathbb{R}^{mN\times nN}, Q\in\mathbb{R}^{m\times n}$. Unitary matrix $I_m=\text{diag}[1,1,\cdots,1]\in\mathbb{R}^{m\times m}$. $\mathcal{Q}>0$ (<0) represents a positive (an negative) definite matrix. $\lambda_{\min}=(\mathcal{Q})$ and $\lambda_{\max}=(\mathcal{Q})$ respectively refer to minimum and maximum eigenvalues of $\mathcal{Q}$, and $\lambda_i(\mathcal{Q})$ denotes $i-$th eigenvalue of $\mathcal{Q}$.

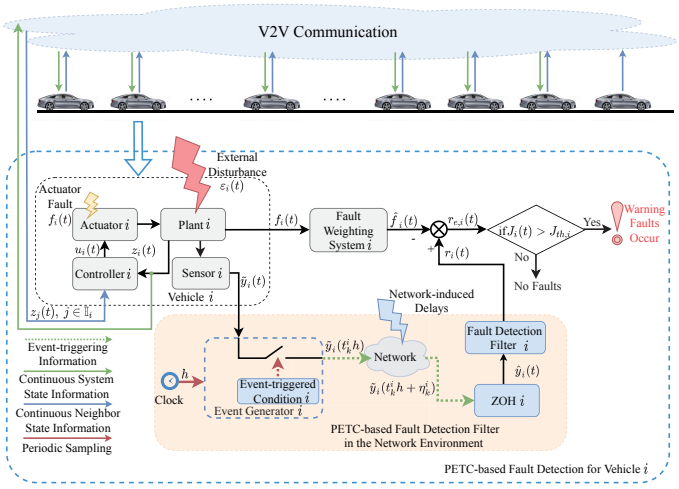

Fig. 1. A framework of network-based fault detection with PETS for a vehicle platoon subject to external disturbances and actuator faults.

II. Problem Formulation

A. Longitudinal Vehicle Dynamics

We take a vehicle platooning system composed of 1 leader and N followers into consideration, which are respectively indexed by 0 and $1,2,\cdots,N$. Here, we exploit a first-order model to characterize the vehicles' longitudinal acceleration behavior:

$$\tau\dot{a}_i(t)+a_i(t)=u_i(t)+\varepsilon_i(t),\ i\in\{1,\cdots,N\}, \tag{1}$$

where $a_i(t)\in\mathbb{R}$ refers to the acceleration of vehicle i. $\tau>0$ denotes the inertial time lag in the powertrain. $u_i(t)\in\mathbb{R}$ refers to the desired control input of vehicle i. $\varepsilon_i(t)\in\mathbb{R}$ stands for the external disturbance (e.g., wind guest, road slope, and lead vehicle's acceleration [33]) on vehicle i, which belongs to $\Lambda_2[0,\infty)$. The model is extensively applied to the basis of platoon control design and analysis [34], [35].

Considering that there is a potential actuator fault in each vehicle, a third-order state-space model for each vehicle under platoon control can be described as follows:

$$\begin{aligned}\dot{z}_i(t) &= Az_i(t)+Bu_i(t)+B\varepsilon_i(t)+Df_i(t),\\ y_i(t) &= Cz_i(t),\end{aligned} \tag{2}$$

where $z_i(t) = [p_i(t), v_i(t), a_i(t)]^T \in \mathbb{R}^3$ refers to the state of vehicle i, $A = \begin{bmatrix} 0 & 1 & 0 \\ 0 & 0 & 1 \\ 0 & 0 & -\frac{1}{\tau} \end{bmatrix}$, $B = \left[0, 0, \frac{1}{\tau}\right]^T$, $f_i(t) \in \mathbb{R}^2$ denotes the actuator fault to be estimated, which means that the velocity and acceleration of vehicle i are influenced and belongs to $\Lambda_2[0, \infty)$, $D \in \mathbb{R}^{3\times 2}$ is a known constant matrix, $y_i(t) \in \mathbb{R}^3$ stands for the measured output, $C = \text{diag}\,[1, 1, 1] \in \mathbb{R}^{3\times 3}$ presents the measured output matrix, which means that position, velocity, and acceleration are measurable.

Note that model (2) and its variants are widely considered as a basis for theoretical analysis of numerous vehicle platoon applications, such as [3], [4], [28], [29], [33], [38], [46].

B. Communication Topology

$\mathcal{G} = (\mathcal{V}, \mathcal{E}, \mathcal{A})$ indicates a directed graph corresponding to the communication topology among N following vehicles (nodes), where $\mathcal{V} = \{1, \cdots, N\}$ and $\mathcal{E} \subseteq \mathcal{V} \times \mathcal{V}$ respectively refer to a node set and an edge set standing for the connections between two following vehicles, and an adjacency matrix $\mathcal{A} = [a_{ij}] \in \mathbb{R}^{N\times N}$ has the following definition:

$$a_{ij} = \begin{cases} 1, & \{v_j, v_i\} \in \mathcal{E}, \\ 0, & \text{otherwise}, \end{cases}$$

where $i, j \in \{1, 2, \cdots, N\}$, $\{v_j, v_i\} \in \mathcal{E}$ implies that vehicle i can receive the information of vehicle j. $\mathbb{N}_i = \{j | a_{ij} = 1\}$ is the neighbor set of vehicle i. Besides, there exists no self-loop in $\mathcal{G}$, *i.e.*, $a_{ii} = 0, \forall i \in \{1, 2, \cdots, N\}$ in this study.

The Laplacian matrix associated with $\mathcal{G}$ is denoted as $\mathcal{L} = [l_{ij}] \in \mathbb{R}^{N\times N}$ with

$$l_{ij} = \begin{cases} -a_{ij}, & i \neq j, \\ \sum_{j\in\mathcal{V}} a_{ij}, & i = j, \end{cases}$$

where $i, j \in \{1, \cdots, N\}$.

In addition, a pinning matrix $\mathcal{M} = \text{diag}\,[\bar{m}_{11}, \bar{m}_{22}, \cdots, \bar{m}_{NN}] \in \mathbb{R}^{N\times N}$ is denoted to indicate the links between the leading and following vehicles, in which $\bar{m}_{ii} = 1$ indicates that vehicle i can receive the information from the leader, and $\bar{m}_{ii} = 0$ otherwise. Next, the leader accessible set of vehicle i has the following definition:

$$\mathbb{M}_i = \begin{cases} \{0\}, & \text{if } \bar{m}_{ii} = 1, \\ \emptyset, & \text{if } \bar{m}_{ii} = 0. \end{cases}$$

In this paper, we mainly pay attention to undirected communication topologies for a vehicle platooning system (See Fig. 2), that is, $i \in \mathbb{N}_j \Leftrightarrow j \in \mathbb{N}_i$ for any $i, j \in \mathcal{V}$, and we assume that undirected communication topologies are connected [34].

III. Design of Network-based Fault Detection Filter with PETC

This section respectively designs a distributed controller to guarantee the string stability of the vehicle platooning system, together with proposing a PETS and devising a PETS-based fault detection filter to generate the residual signal for fault detection. Then, a reference fault weighting system is given to acquire better performance. Moreover, by combining the vehicle platoon, the fault detection filter, and the reference fault weighting system, a residual system of fault detection is constructed to guarantee the design of the fault detection filter.

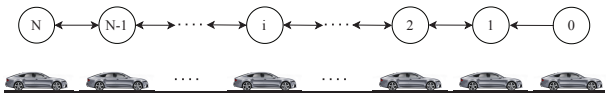

Fig. 2. Example of undirected communication topology for a vehicle platooning system.

A. Design of Distributed Controller

Considering that each vehicle can only utilize its neighborhood information denoted as $\mathbb{I}_i = \mathbb{M}_i \bigcup \mathbb{N}_i$, we focus on a linear distributed controller satisfying string stability as follows [36]:

$$u_i(t) = -\sum_{j\in\mathbb{I}_i} [k_p(p_i - p_j - d_{i,j}) + k_v(v_i - v_j) + k_a(a_i - a_j)], \quad (3)$$

where k_p, k_v, and k_a are the controller gains to be designed.

Denote the state of the leading vehicle as $z_0(t) = [p_0, v_0, a_0]^T$ which satisfies $\dot{z}_0(t) = Az_0(t)$, then the tracking error of vehicle i has the following definition:

$$\begin{cases} \tilde{p}_i(t) &= p_i - p_0 - d_{0,i} = p_i - p_0 - \sum_{j=0}^{i-1} d_{j,j+1}, \\ \tilde{v}_i(t) &= v_i - v_0, \\ \tilde{a}_i(t) &= a_i - a_0. \end{cases}$$

According to the above equation, (3) can be rewritten as

$$u_i(t) = -\sum_{j\in\mathbb{I}_i} [k_p(\tilde{p}_i - \tilde{p}_j) + k_v(\tilde{v}_i - \tilde{v}_j) + k_a(\tilde{a}_i - \tilde{a}_j)], \quad (4)$$

then to guarantee the string stability of the vehicle platoon subjected to external disturbances and actuator faults, this paper will design corresponding controller gains in distributed controller (4) according to [46].

Remark 1: There exist two types of spacing policies extensively applied in the vehicle platoon, that is, the constant time headway (CTH) policy and the constant spacing (CS) policy [37], [38]. Considering that this study aims to investigate fault detection for a vehicle platooning system, a simpler CS policy is applied in the vehicle platoon.

For the sake of the following analysis, the state of tracking error $\tilde{z}_i(t)$ satisfies $\tilde{z}_i(t) = [\tilde{p}_i(t), \tilde{v}_i(t), \tilde{a}_i(t)]^T$, resulting in the following representation of distributed controller (4): $u_i(t) = -K\sum_{j\in\mathbb{I}_i}(\tilde{z}_i(t) - \tilde{z}_j(t))$, where $K = (k_p, k_v, k_a)$. Then, the closed-loop dynamics of vehicle i have the following expression:

$$\begin{aligned} \dot{\tilde{z}}_i(t) &= A\tilde{z}_i(t) - BK\left[\sum_{j=1}^{N} a_{ij}(\tilde{z}_i(t) - \tilde{z}_j(t)) + \bar{m}_{ii}\tilde{z}_i(t)\right] \\ &\quad + B\varepsilon_i(t) + Df_i(t), \\ \tilde{y}_i(t) &= C\tilde{z}_i(t), \end{aligned} \quad (5)$$

where $\tilde{y}_i(t) \in \mathbb{R}^3$ is the output of closed-loop system (5).

B. Design of Event Generator

For saving limited network and communication resources and decreasing bandwidth utilization, an event generator is devised for the vehicle platoon. The transmission instant set of vehicle i is presented as $\{t_k^i h | t_k^i \in \mathbb{N}\}$, in which t_k^i is

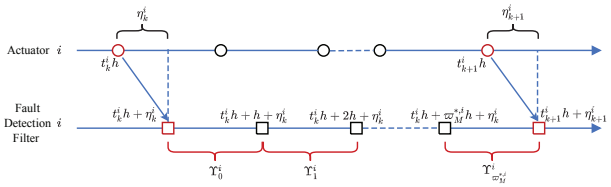

Fig. 3. Signal transmission for the controlled vehicle platoon through the network.

determined by the following condition of output-based PETS [30], [31]:

$$t_{k+1}^i = t_k^i + \min_{l\in\mathbb{Z}^+}\{l|\Xi_{\tilde{y}_i}^T \kappa \Xi_{\tilde{y}_i} > \delta_i \tilde{y}_i^T(\rho_i h)\kappa\tilde{y}_i(\rho_i h)\}, \quad (6)$$

with $\Xi_{\tilde{y}_i} = \tilde{y}_i(\rho_i h) - \tilde{y}_i(t_k^i h)$, $0 < \delta_i \in \mathbb{R}$ is a given threshold parameter, $\rho_i h = t_k^i h + lh$, and weight matrix $0 < \kappa \in \mathbb{R}^{3\times 3}$ need to be designed.

According to (6), the minimum inter-event time can be determined by $h > 0$, which implies that Zeno behavior is avoided effectively. Due to the behavior of zero-order-holder (ZOH) and network-induced delay (see Fig. 3), we define an output of ZOH $\hat{y}_i(t)$ as follows:

$$\hat{y}_i(t) = \tilde{y}_i(t_k^i h), \quad t \in [t_k^i h + \eta_k^i, t_{k+1}^i h + \eta_{k+1}^i), \quad (7)$$

where $\eta_k^i > 0$ stands for the transmission delay and $\eta_m^i \leqslant \eta_k^i \leqslant \eta_M^i$.

Denote the following subintervals on $t \in [t_k^i h + \eta_k^i, t_{k+1}^i h + \eta_{k+1}^i)$:

$$\begin{cases} \Upsilon_0^i & = [t_k^i h + \eta_k^i, t_k^i h + h + \eta_k^i), \\ \Upsilon_1^i & = [t_k^i h + h + \eta_k^i, t_k^i h + 2h + \eta_k^i), \\ & \vdots \\ \Upsilon_{\varpi_M^{*,i}}^i & = [t_k^i h + \varpi_M^{*,i} h + \eta_k^i, t_{k+1}^i h + \eta_{k+1}^i), \end{cases}$$

with $\varpi_M^{*,i} = \min\{\varpi | t_k^i h + (\varpi+1)h + \eta_k^i \geqslant t_{k+1}^i h + \eta_{k+1}^i\}$.

Error vector $e_i(t) \in \mathbb{R}^3$ and piecewise time-varying delay $\tau_i(t)$ have the following definition:

$$e_i(t) = \begin{cases} \tilde{y}_i(t_k^i h) - \tilde{y}_i(t_k^i h), & t \in \Upsilon_0^i, \\ \vdots & \vdots \\ \tilde{y}_i(t_k^i h + \varpi_M^* h) - \tilde{y}_i(t_k^i h), & t \in \Upsilon_{\varpi_M^{*,i}}^i, \end{cases}$$

$$\tau_i(t) = \begin{cases} t - t_k^i h, & t \in \Upsilon_0^i, \\ \vdots & \vdots \\ t - t_k^i h - \varpi_M^{*,i} h, & t \in \Upsilon_{\varpi_M^{*,i}}. \end{cases}$$

Note that $\tau_i(t)$ is a time-varying artificial delay rather than network-induced delay. Therefore, output of ZOH $\hat{y}_i(t)$ can be redefine as

$$\hat{y}_i(t) = \tilde{y}_i(t_k^i h) = \tilde{y}_i(t - \tau_i(t)) - e_i(t). \quad (8)$$

Denote $\tau_m^i = \eta_m^i$, $\tau_M^i = h + \eta_M^i$, and $d^i = \tau_M^i - \tau_m^i$. It follows that $\tau_m^i \leqslant \tau_i(t) \leqslant \tau_M^i$.

Remark 2: More recently, as an economic and useful strategy to save communication and network resources, the ETS has been successfully applied in various fields such as academics and engineering. Considering that a vehicle platoon can receive and exchange some necessary information based on network and vehicle-to-vehicle (V2V) communication, which may be limited by bandwidth and resources of communication in many scenarios, it is beneficial to use the ETS to investigate fault detection for a vehicle platooning system based on the condition of the network and V2V communication. Furthermore, the general ETS needs to devise a minimum triggered interval to avoid Zeno behavior and require continuous monitoring of a triggering condition, which may waste numerous network and communication resources. Given this, some scholars have further proposed a PETS to overcome that disadvantage, and plentiful results have been obtained. Therefore, it is meaningful to utilize the PETS to discuss this topic.

C. Design of Fault Detection Filter

It should be mentioned that there exist some inevitable factors, e.g., zero shift, network disturbance, and aging, which may cause the actuator fault, e.g., enlarging, tightening, and no output, for a vehicle platoon. In what follows, to judge whether or not vehicle faults have happened, we design a fault detection filter with the PETS, which includes a residual generator to generate the needed residual signal. The fault detection filter for each follower in the vehicle platoon is formulated as follows:

$$\begin{aligned} \dot{\hat{z}}_i(t) &= A_f \hat{z}_i(t) + B_f \hat{y}_i(t), \\ r_i(t) &= C_f \hat{z}_i(t) + D_f \hat{y}_i(t), \end{aligned} \quad (9)$$

where $\hat{z}_i(t) \in \mathbb{R}^4$ refers to the filter state vector. $r_i(t) \in \mathbb{R}$ denotes the residual signal, and $\hat{y}_i(t)$ indicates the input of the fault detection filter of each vehicle (which is influenced by the PETS). The filter matrices A_f, B_f, C_f, and D_f have suitable dimensions and are designed later.

For obtaining better performance, we define a reference model as $\hat{f}(s) = \Theta(s)f(s)$, where $\Theta(s)$ stands for a stable weighting matrix [39]. The minimal state-space realization of $\Theta(s)$ has the following definition

$$\begin{aligned} \dot{z}_{w,i}(t) &= A_w z_{w,i}(t) + B_w f_i(t), \\ \hat{f}_i(t) &= C_w z_{w,i}(t) + D_w f_i(t), \end{aligned} \quad (10)$$

where $z_{w,i}(t) \in \mathbb{R}$ refers to the state vector of the system. Some constant matrices A_w, B_w, C_w, and D_w are known and predefined. $\hat{f}_i(t) \in \mathbb{R}$ indicates the weighting fault signal. In addition, a framework of network-based fault detection is exhibited in Fig. 1 for a vehicle platooning system.

Accordingly, closed-loop system (5), fault detection filter (9) and fault weighting system (10) can respectively be rewritten as the following representations:

$$\begin{cases} \dot{\tilde{\mathbf{z}}}(t) = [(I_N \otimes A) - (\mathcal{L}+\mathcal{M}) \otimes BK]\tilde{\mathbf{z}}(t) \\ \qquad\qquad + (I_N \otimes B)\boldsymbol{\varepsilon}(t) + (I_N \otimes D)\mathbf{f}(t), \\ \tilde{\mathbf{y}}(t) = (I_N \otimes C)\tilde{\mathbf{z}}(t), \end{cases}$$

$$\begin{cases} \dot{\mathbf{z}}_w(t) = (I_N \otimes A_w)\mathbf{z}_w(t) + (I_N \otimes B_w)\mathbf{f}(t), \\ \hat{\mathbf{f}}(t) = (I_N \otimes C_w)\mathbf{z}_w(t) + (I_N \otimes D_w)\mathbf{f}(t), \end{cases}$$

$$\begin{cases} \dot{\hat{\mathbf{z}}}(t) = (I_N \otimes A_f)\hat{\mathbf{z}}(t) + (I_N \otimes B_f)\hat{\mathbf{y}}(t), \\ \mathbf{r}(t) = (I_N \otimes C_f)\hat{\mathbf{z}}(t) + (I_N \otimes D_f)\hat{\mathbf{y}}(t), \end{cases}$$

where $\tilde{\mathbf{z}}(t)=(\tilde{z}_1^T(t),\tilde{z}_2^T(t),\cdots,\tilde{z}_N^T(t))^T, \mathbf{f}(t)=(f_1^T(t), f_2^T(t),\cdots,f_N^T(t))^T, \mathbf{z}_w(t)=(z_{w,1}(t),z_{w,2}(t),\cdots z_{w,N}(t))^T, \boldsymbol{\varepsilon}(t)=(\varepsilon_1(t),\varepsilon_2(t),\cdots,\varepsilon_N(t))^T, \hat{\mathbf{f}}(t)=(\hat{f}_1(t),\hat{f}_2(t),\cdots,\hat{f}_N(t))^T, \hat{\mathbf{z}}(t)=(\hat{z}_1^T(t),\hat{z}_2^T(t)\cdots,\hat{z}_N^T(t))^T, \mathbf{r}(t)=(r_1(t), r_2(t),\cdots,r_N(t)), \tilde{\mathbf{y}}(t)=(\tilde{y}_1^T(t),\tilde{y}_2^T(t),\cdots,\tilde{y}_N^T(t))^T, \hat{\mathbf{y}}(t)=(\hat{y}_1^T(t),\hat{y}_2^T(t),\cdots,\hat{y}_N^T(t))^T$.

To guarantee the design of fault detection filter (9), a residual system is defined with its state vector $\mathcal{S}(t)=(\tilde{\mathbf{z}}^T(t),\mathbf{z}_w^T(t),\hat{\mathbf{z}}^T(t))^T\in\mathbb{R}^{8N}$ and expected output $\mathbf{r}_e(t)\in\mathbb{R}^N$, resulting in the following formulation:

$$\begin{aligned}\dot{\mathcal{S}}(t) &= \Phi_1\mathcal{S}(t)+\Phi_2\mathcal{S}(t-\tau(t))+\Phi_3\vartheta(t)+\Phi_4\mathbf{e}(t),\\ \mathbf{r}_e(t) &= \Phi_5\mathcal{S}(t)+\Phi_6\mathcal{S}(t-\tau(t))+\Phi_7\vartheta(t)+\Phi_8\mathbf{e}(t),\end{aligned}\tag{11}$$

where $\mathcal{S}(t)=(\mathcal{S}_1^T(t),\mathcal{S}_2^T(t),\cdots,\mathcal{S}_N^T(t))^T, \mathbf{r}_e(t)=\mathbf{r}(t)-\hat{\mathbf{f}}(t)=(r_{e,1}(t),r_{e,2}(t),\cdots,r_{e,N}(t))^T\in\mathbb{R}^N, \vartheta(t)=(\mathbf{f}^T(t),\boldsymbol{\varepsilon}^T(t))^T\in\mathbb{R}^{3N}, \mathcal{S}(t-\tau(t))=(\mathcal{S}_1^T(t-\tau_1(t)),\mathcal{S}_2^T(t-\tau_2(t)),\cdots,\mathcal{S}_N^T(t-\tau_N(t)))^T, \mathbf{e}(t)=(e_1^T(t),e_2^T(t),\cdots,e_N^T(t))^T\in\mathbb{R}^{3N}, \Phi_1=\mathrm{diag}[\hat{A},I_N\otimes A_w, I_N\otimes A_f], \hat{A}=(I_N\otimes A)-(\mathcal{L}+\mathcal{M})\otimes BK,$

$$\Phi_2=\begin{pmatrix}0_{4N\times 3N} & 0_{4N\times 5N}\\ I_N\otimes(B_fC) & 0_{4N\times 5N}\end{pmatrix}, \Phi_3=\begin{pmatrix}I_N\otimes D & I_N\otimes B\\ I_N\otimes B_w & 0_{N\times N}\\ 0_{4N\times 2N} & 0_{4N\times N}\end{pmatrix},$$

$\Phi_4=(0_{3N\times 4N},-I_N\otimes B_f^T)^T, \Phi_5=(0_{N\times 3N},-I_N\otimes C_w, I_N\otimes C_f), \Phi_6=(I_N\otimes(D_fC),0_{N\times 5N}), \Phi_7=(-I_N\otimes D_w,0_{N\times N}), \Phi_8=-I_N\otimes D_f$.

Then, the definition of H_∞ performance for residual system (11) is given as follows, which is important for the following result.

Definition 1 ($\mathcal{H}_\infty$ Disturbance Attenuation): Residual system (11) is said to be asymptotic stable with a guaranteed H_∞ performance if the following two requirements hold.

1) Residual system (11) can achieve asymptotic stability with $\vartheta(t)=0$.

2) Under zero initial conditions, residual system (11) fulfills an H_∞ performance with a disturbance attenuation level ζ, if

$$\int_0^\infty \mathbf{r}_e^T(\omega)\mathbf{r}_e(\omega)d\omega\leqslant\zeta^2\int_0^\infty\vartheta^T(\omega)\vartheta(\omega)d\omega\tag{12}$$

for all nonzero $\vartheta(t)\in\Lambda_2$.

This paper aims to tackle the design of PETS-based fault detection filter (9) in vehicle platoon (2), which carries out in the following two steps:

1) Produce the residual signal: for vehicle platoon (1), devise fault detection filter (9) with the PETS for each vehicle to generate residual signals. Moreover, the devised fault detection filter can ensure that residual system (11) fulfills asymptotic stability with H_∞ performance (12).
2) Formulate a fault detection measure: after the fault detection filter for vehicle platoon (1) are designed, by using the strategy proposed in [40], residual evaluation functions $J_i(t)$ and thresholds $J_{th,i}$ have the following definitions:

$$\begin{aligned}J_i(t) &= \sqrt{\frac{1}{t}\int_0^t r_i^T(\omega)r_i(\omega)d\omega},\ i=1,2,\cdots,N,\\ J_{th,i} &= \sup_{\varepsilon_i(t)\in\Lambda_2, f_i(t)=0} J_i(t).\end{aligned}\tag{13}$$

Next, the fault detection criterion is as follows:

$$\begin{cases}J_i(t)>J_{th,i}\Rightarrow\text{faults occur}\Rightarrow\text{alarm},\\ J_i(t)\leqslant J_{th,i}\Rightarrow\text{no faults}.\end{cases}$$

IV. Stability with H_∞ Performance Analysis of the Residual System

In this section, we develop several sufficient conditions to ensure the stability of the residual system with H_∞ performance by formulating the Lyapunov-Krasovskii functional and inequality techniques. Before we present theorems of stability with H_∞ performance for this system, some essential lemmas are given to ensure the following proof of our works.

Lemma 1 (see [41]): For an integrable function $\{S(u)|u\in[\sigma_1,\sigma_2]\}$ and a matrix $0<Q\in\mathbb{R}^{n\times n}$, the following inequality holds:

$$\begin{aligned}&-\int_{\sigma_1}^{\sigma_2}S^T(\omega)QS(\omega)d\omega\\ \leqslant\ &\frac{1}{\sigma_1-\sigma_2}\left(\int_{\sigma_1}^{\sigma_2}S(\omega)d\omega\right)^TQ\left(\int_{\sigma_1}^{\sigma_2}S(\omega)d\omega\right).\end{aligned}$$

Lemma 2 (see [42]): Let $S(t)\in\mathcal{Y}[\sigma_1,\sigma_2)$ and $S(\sigma_1)=0$. Then for any matrix $0<Q\in\mathbb{R}^{n\times n}$, the following inequality holds:

$$\int_{\sigma_1}^{\sigma_2}S^T(\omega)QS(\omega)d\omega\leqslant\frac{4(\sigma_2-\sigma_1)^2}{\pi^2}\int_{\sigma_1}^{\sigma_2}\dot{S}^T(\omega)Q\dot{S}(\omega)d\omega.$$

Lemma 3 (see [43]): For a vector function $\dot{S}:[-\tau,0]\to\mathbb{R}^n$, scalar $0\leqslant\tau(t)\leqslant\tau$, and any matrix $L>0, \mathcal{W}=\begin{pmatrix}L & H\\ * & L\end{pmatrix}\geqslant 0$ such that the integration in the following inequality is well defined, it holds

$$-\tau\int_{t-\tau}^t\dot{S}^T(\omega)L\dot{S}(\omega)d\omega\leqslant\hat{S}^T(t)Q\hat{S}(t),$$

where $\hat{S}^T(t)=[S^T(t),S^T(t-\tau(t)),S^T(t-\tau)]$, $Q=\begin{pmatrix}-L & L-H & H\\ * & [H-L]_s & L-H\\ * & * & -L\end{pmatrix}$.

Accordingly, to ensure that residual system (11) can achieve H_∞ asymptotic stability, a theorem condition is provided, resulting in the following representation:

Theorem 1: If there exist positive matrices $P,Q_1,Q_2,R_1,R_2,E,\kappa,G$ with $\begin{pmatrix}R_2 & G\\ * & R_2\end{pmatrix}>0$, constant matrices A_f,B_f,C_f,D_f, and constant ζ such that the following inequality holds

$$\Psi_1=\begin{pmatrix}\Psi_4 & \tilde{\Phi}_1 & \tilde{\Phi}_2 & \tilde{\Phi}_3 & \hat{\Phi}_1^T\\ * & -\hat{\tilde{R}}_1 & \tilde{0} & \tilde{0} & \check{0}\\ * & * & -\hat{\tilde{R}}_2 & \tilde{0} & \check{0}\\ * & * & * & -\hat{\tilde{E}} & \check{0}\\ * & * & * & * & -I_N\end{pmatrix}<0,\tag{14}$$

where

$$\begin{aligned}
\check{0} &= 0_{8N\times N}, \tilde{0} = 0_{8N\times 8N}, \bar{0} = 0_{8N\times 3N}, \hat{0} = 0_{3N\times 3N},\\
\tilde{E} &= \epsilon^T E\epsilon, \tilde{G} = \epsilon^T G\epsilon, \tilde{Q}_1 = \epsilon^T Q_1\epsilon, \tilde{Q}_2 = \epsilon^T Q_2\epsilon,\\
\tilde{R}_1 &= \epsilon^T R_1\epsilon, \tilde{R}_2 = \epsilon^T R_2\epsilon, \epsilon = (I_4, 0_{4\times 4}), \hat{\kappa} = I_N\otimes\kappa,\\
\chi_{11} &= I_N\otimes\tilde{Q}_1 - I_N\otimes\tilde{R}_1 + [P\Phi_1]_s - \frac{\pi^2}{4}(I_N\otimes\tilde{E}),\\
\chi_{23} &= I_N\otimes(\tilde{R}_2-\tilde{G}), \chi_{13} = \frac{\pi^2}{4}(I_N\otimes\tilde{E}) + P\Phi_2,\\
\chi_{22} &= I_N\otimes(\tilde{Q}_2-\tilde{Q}_1-\tilde{R}_1-\tilde{R}_2), \chi_{15} = P\Phi_3,\\
\chi_{33} &= -\frac{\pi^2}{4}(I_N\otimes\tilde{E}) + I_N\otimes([\tilde{G}-\tilde{R}_2]_s) + \tilde{C}^T(\delta\otimes\kappa)\tilde{C},\\
\Psi_4 &= \begin{pmatrix} \chi_{11} & I_N\otimes\tilde{R}_1 & \chi_{13} & \tilde{0} & \chi_{15} & \chi_{16}\\ * & \chi_{22} & \chi_{23} & I_N\otimes\tilde{G} & \bar{0} & \bar{0}\\ * & * & \chi_{33} & \chi_{23} & \bar{0} & \bar{0}\\ * & * & * & \chi_{44} & \bar{0} & \bar{0}\\ * & * & * & * & \chi_{55} & \hat{0}\\ * & * & * & * & * & -\hat{\kappa}\end{pmatrix},\\
\chi_{44} &= -I_N\otimes(\tilde{Q}_2+\tilde{R}_2), \tilde{C} = I_N\otimes(0_{3\times 1}, C, 0_{3\times 4}),\\
\chi_{16} &= P\Phi_4, I_{2N} = (I_N\otimes I_2), \chi_{55} = -\zeta^2 I_{3N},\\
\hat{\Phi}_1 &= (\Phi_5, 0_{N\times 8N}, \Phi_6, 0_{N\times 8N}, \Phi_7, \Phi_8),\\
\tilde{\Phi}_1 &= \tilde{\Phi}^T(I_N\otimes(\epsilon^T R_1)), \tilde{\Phi}_2 = \tilde{\Phi}^T(I_N\otimes(\epsilon^T R_2)),\\
\tilde{\Phi}_3 &= \tilde{\Phi}^T(I_N\otimes(\epsilon^T E)), \delta = \mathrm{diag}[\delta_1, \delta_2, \cdots, \delta_N],\\
\tilde{\Phi} &= (\Phi_1, 0_{8N\times 8N}, \Phi_2, 0_{8N\times 8N}, \Phi_3, \Phi_4),\\
d^2 &= \mathrm{diag}[(d_1^2)^2, (d_2^2)^2, \cdots, (d_N^2)^2], \hat{\bar{R}}_2 = (d^2)^{-1}\otimes R_2,\\
\tau_m^2 &= \mathrm{diag}[(\tau_m^1)^2, (\tau_m^2)^2, \cdots, (\tau_m^N)^2], \hat{\bar{R}}_1 = (\tau_m^2)^{-1}\otimes R_1,\\
\tau_M^2 &= \mathrm{diag}[(\tau_M^1)^2, (\tau_M^2)^2, \cdots, (\tau_M^N)^2], \hat{\bar{E}} = (\tau_M^2)^{-1}\otimes E,
\end{aligned}$$

then residual system (11) achieves asymptotic stability with H_∞ performance (12).

Proof: See Appendix A.

It should be mentioned that Theorem 1 cannot be resolved by utilizing the LMI toolbox since residual system (17) is coupled with an unknown matrix P. Consequently, inspired by [33], the following theorem can be formulated to address the above issue:

Theorem 2: If there exist positive matrices $\hat{P}_1, Q_1, Q_2, R_1, R_2, E, \kappa, G, \Gamma$ with $\begin{pmatrix} R_2 & G\\ * & R_2\end{pmatrix} > 0$, constant matrices $\hat{A}_f, \hat{B}_f, \hat{C}_f, \hat{D}_f$, and constant ζ such that the following inequality holds

$$\hat{\Psi}_1 = \begin{pmatrix} \hat{\Psi}_4 & \hat{\bar{\Phi}}_1 & \hat{\bar{\Phi}}_2 & \hat{\bar{\Phi}}_3 & \hat{\bar{\Phi}}_2^T\\ * & -\hat{\bar{R}}_1 & \tilde{0} & \tilde{0} & \check{0}\\ * & * & -\hat{\bar{R}}_2 & \tilde{0} & \check{0}\\ * & * & * & -\hat{\bar{E}} & \check{0}\\ * & * & * & * & -I_N\end{pmatrix} < 0, \qquad (15)$$

where

$$\hat{\Psi}_4 = \begin{pmatrix} \hat{\chi}_{11} & \hat{R}_1 & \hat{\chi}_{13} & \hat{\bar{0}} & \hat{\chi}_{15} & \hat{\chi}_{16}\\ * & \hat{\chi}_{22} & \hat{\chi}_{23} & I_N\otimes G & \hat{\bar{0}} & \hat{\bar{0}}\\ * & * & \hat{\chi}_{33} & \hat{\chi}_{23} & \hat{\bar{0}} & \hat{\bar{0}}\\ * & * & * & \hat{\chi}_{44} & \hat{\bar{0}} & \hat{\bar{0}}\\ * & * & * & * & \chi_{55} & \hat{0}\\ * & * & * & * & * & -\hat{\kappa}\end{pmatrix},$$

$$\begin{aligned}
\hat{\chi}_{11} &= \begin{pmatrix} \bar{\chi}_{11} & \bar{A}_f + \bar{A}^T\Gamma\\ * & \bar{A}_f + \bar{A}_f^T\end{pmatrix}, \hat{R}_1 = \begin{pmatrix} I_N\otimes R_1\\ \hat{\bar{0}}\end{pmatrix},\\
\bar{\chi}_{11} &= I_N\otimes(Q_1 - R_1 - \frac{\pi^2}{4}E) + [(I_N\otimes\hat{P}_1)\bar{A}]_s\\
\bar{A} &= \mathrm{diag}[I_N\otimes A - (\mathcal{L}+\mathcal{M})\otimes BK, I_N\otimes A_w],\\
\Gamma &= (I_N\otimes(\hat{P}_2\hat{P}_3^{-1})), \bar{A}_f = I_N\otimes\hat{A}_f, \hat{\bar{0}} = 0_{4N\times 3N},\\
\hat{\bar{0}} &= 0_{4N\times 4N}, \hat{\Phi}_2 = (\bar{B}_f(I_N\otimes C), 0_{4N\times N}),\\
\hat{\chi}_{22} &= I_N\otimes(Q_2 - Q_1 - R_1 - R_2), \hat{\chi}_{23} = I_N\otimes(R_2 - G),\\
\hat{\chi}_{33} &= -\frac{\pi^2}{4}(I_N\otimes E) + I_N\otimes([G-R_2]_s) + \bar{C}^T(\delta\otimes\kappa)\bar{C},\\
\hat{\chi}_{13} &= \begin{pmatrix} \frac{\pi^2}{4}(I_N\otimes E) + \hat{\Phi}_2\\ \hat{\Phi}_2\end{pmatrix}, \hat{\chi}_{15} = \begin{pmatrix} (I_N\otimes\hat{P}_1)\hat{\Phi}_3\\ \Gamma\hat{\Phi}_3\end{pmatrix},\\
\hat{\Phi}_3 &= \begin{pmatrix} I_N\otimes D & I_N\otimes B\\ I_N\otimes B_w & 0_{N\times N}\end{pmatrix}, \hat{\chi}_{16} = \begin{pmatrix} -\bar{B}_f\\ -\bar{B}_f\end{pmatrix},\\
\hat{\chi}_{44} &= -I_N\otimes(Q_2+R_2), \bar{C} = I_N\otimes(0_{3\times 1}, C),\\
\hat{\Phi}_6 &= (I_N\otimes(\hat{D}_f C), 0_{N\times 5N}), \bar{B}_f = (I_N\otimes\hat{B}_f),\\
\hat{\bar{\Phi}}_2 &= (\hat{\Phi}_5, 0_{N\times 3N}, \hat{\Phi}_6, 0_{N\times N}, \Phi_7, \hat{\Phi}_8),\\
\hat{\Phi}_5 &= (0_{N\times 3N}, -I_N\otimes C_w, I_N\otimes\hat{C}_f), \hat{\Phi}_8 = -I_N\otimes\hat{D}_f,\\
\hat{\bar{\Phi}}_1 &= \hat{\bar{\Phi}}^T(I_N\otimes R_1), \hat{\bar{\Phi}}_2 = \hat{\bar{\Phi}}^T(I_N\otimes R_2),\\
\hat{\bar{\Phi}}_3 &= \hat{\bar{\Phi}}^T(I_N\otimes E), \hat{\bar{\Phi}} = (\bar{A}, 0_{4N\times 16N}, \hat{\Phi}_3, 0_{4N\times 3N}),
\end{aligned}$$

then residual system (11) achieves asymptotic stability with H_∞ performance (12).

Proof: See Appendix B.

It should be noticed that (15) will have a very high dimension with the number of following vehicles increasing, even rendering the issue intractable. Inspired by [33], condition (15) is decomposed for individual vehicles such that it can be efficiently solved.

Theorem 3: If there exist positive matrices $\hat{P}_1, Q_1, Q_2, R_1, R_2, E, \kappa, G, \hat{\Gamma}$ with $\begin{pmatrix} R_2 & G\\ * & R_2\end{pmatrix} > 0$, constant matrices $\hat{A}_f, \hat{B}_f, \hat{C}_f, \hat{D}_f$, and constant ζ such that the following inequality holds

$$\hat{\Psi}_{2,i} = \begin{pmatrix} \bar{\Psi}_{5,i} & \bar{\Phi}_{1,i} & \bar{\Phi}_{2,i} & \bar{\Phi}_{3,i} & \bar{\hat{\Phi}}_3^T\\ * & -\frac{R_1}{(\tau_m^i)^2} & \tilde{0} & \tilde{0} & \check{0}\\ * & * & -\frac{R_2}{(d^i)^2} & \tilde{0} & \check{0}\\ * & * & * & -\frac{E}{(\tau_M^i)^2} & \check{0}\\ * & * & * & * & -I\end{pmatrix} < 0, \qquad (16)$$

where $i = 1, 2, \cdots, N$,

$$\begin{aligned}
\bar{\Psi}_{5,i} &= \begin{pmatrix} \bar{\chi}_{11} & \hat{\bar{R}}_1 & \bar{\chi}_{13} & 0_{4\times 4} & \bar{\chi}_{15} & \bar{\chi}_{16}\\ * & \bar{\chi}_{22} & \bar{\chi}_{23} & G & 0_{4\times 3} & 0_{4\times 3}\\ * & * & \bar{\chi}_{33} & \bar{\chi}_{23} & 0_{4\times 3} & 0_{4\times 3}\\ * & * & * & \bar{\chi}_{44} & 0_{4\times 3} & 0_{4\times 3}\\ * & * & * & * & -\zeta^2 I_3 & 0_{3\times 3}\\ * & * & * & * & * & -\kappa\end{pmatrix},\\
\bar{\chi}_{11,i} &= \begin{pmatrix} Q_1 - R_1 - \frac{\pi^2}{4}E + [\hat{P}_1\tilde{A}_i]_s & \hat{A}_f + \tilde{A}^T\hat{\Gamma}\\ * & \hat{A}_f + \hat{A}_f^T\end{pmatrix},\\
\tilde{A}_i &= \mathrm{diag}[A - \varsigma_i BK, A_w], \varsigma_i = \lambda_i(\mathcal{L}+\mathcal{M}),
\end{aligned}$$

$$\begin{aligned}
\hat{\bar{R}}_1 &= \begin{pmatrix} R_1 \\ 0_{4\times4} \end{pmatrix}, \bar{\chi}_{13} = \begin{pmatrix} \frac{\pi^2}{4}E + \hat{\bar{\Phi}}_2 \\ \hat{\bar{\Phi}}_2 \end{pmatrix}, \hat{\bar{\Phi}}_2 = (\hat{B}_f C, 0_{4\times1}), \\
\bar{\chi}_{16} &= \begin{pmatrix} -\hat{B}_f \\ -\hat{B}_f \end{pmatrix}, \bar{\chi}_{15} = \begin{pmatrix} \hat{P}_1\hat{\bar{\Phi}}_3 \\ \hat{\Gamma}\hat{\bar{\Phi}}_3 \end{pmatrix}, \hat{\bar{\Phi}}_3 = \begin{pmatrix} D & B \\ B_w & 0 \end{pmatrix}, \\
\hat{\Gamma} &= \hat{P}_2\hat{P}_3^{-1}, \bar{\chi}_{22} = (Q_2 - Q_1 - R_1 - R_2), \bar{\chi}_{23} = (R_2 - G), \\
\bar{\chi}_{33,i} &= -\frac{\pi^2}{4}E + ([G - R_2]_s) + \delta_i \hat{\bar{C}}^T \kappa \hat{\bar{C}}, \bar{\chi}_{44} = -Q_2 - R_2, \\
\hat{\bar{C}} &= (0_{3\times1}, C), \bar{\Phi}_5 = (0_{1\times3}, -C_w, \hat{C}_f), \\
\bar{\Phi}_6 &= (\hat{D}_f C, 0_{1\times5}), \bar{\Phi}_7 = (-D_w, 0), \bar{\Phi}_8 = -\hat{D}_f, \\
\hat{\bar{\Phi}}_3 &= (\bar{\Phi}_5, 0_{1\times3}, \bar{\Phi}_6, 0, \bar{\Phi}_7, \bar{\Phi}_8), \bar{\Phi}_{1,i} = \bar{\Phi}_i^T R_1, \\
\bar{\Phi}_{2,i} &= \bar{\Phi}_i^T R_2, \bar{\Phi}_{3,i} = \bar{\Phi}_i^T E, \bar{\Phi}_i = (\tilde{A}_i, 0_{4\times16}, \hat{\bar{\Phi}}_3, 0_{4\times3})
\end{aligned}$$

for all $\varsigma_i = \lambda_i(\mathcal{L}+\mathcal{M})$, $i = 1, 2, \cdots, N$, then residual system (11) achieves asymptotic stability with H_∞ performance (12).

Proof: See Appendix C.

Remark 3. Compared with (15), (16) only has the size of an individual vehicle. It decreases computational complexity and saves more computational resources. Moreover, $\hat{\Psi}_{2,i}, i = 1, 2, \cdots, N$ is affine in ς_i, condition (16) holds when and only when it holds for the minimum and maximum eigenvalue of $\mathcal{L} + \mathcal{M}$ [33]. In addition, compared with our previous works about the PETS-based controller [32], [44] and the PETS-based H_∞ filter [45], this paper not only extends to the case of the PETS-based fault detection filter but also employs a useful approach to decrease the dimensions of Theorem conditions.

V. Numerical Experiments and Field Experiments

In this section, numerical experiments and field experiments are presented to testify the validity of the presented theorems.

A. Numerical Experiments

TABLE I
Parameters of Numerical Experiments.

Symbol	Unit	Value (i is the vehicle index)
τ	s	0.1
$d_{0,i}$	m	$i \times 10$
δ_i	-	0.2
k_p	-	5
k_v	-	6
k_a	-	1
$\eta_{M,i}$	ms	40
$\eta_{m,i}$	ms	10

If not elsewhere specified, the platoon is composed of one leading and eight following vehicles through V2V communication in numerical experiments. We select $D = \begin{pmatrix} 0 & 1 & 0 \\ 0 & 0 & 1 \end{pmatrix}^T$ that accounts for actuator faults that affect the velocity and acceleration response, then inertial lag, the threshold parameter, desired inter-vehicle distance, and distributed feedback gains are shown in Table I, where selecting controller parameters can ensure the string stability of the vehicle platoon considered in this paper (see [46]). $\eta_i \in [\eta_{m,i}, \eta_{M,i}]$ implies a delay induced by the network and exhibits in Table I. Moreover, we choose the following parameters for the fault weighting system [43]:

$$A_w = -0.1, B_w = (0.25\ 0.75), C_w = 0.5, D_w = (0\ 0).$$

Then, three cases are respectively presented as follows.

Case I: A fault-free vehicle platoon

In this case, we select the leader vehicle's initial state as $z_0(0) = (0, 14, 0)^T$ and eight following vehicles as $z_i(0) = (-10i, \cos(i)+15, 0), i = 1, 2, \cdots, 8$, and external disturbance $\varepsilon_i(t) = \begin{cases} 0.1\sin(t), & t \in [5\text{s}, 30\text{s}], \\ 0, & \text{otherwise.} \end{cases}$ Then, Fig. 4 (a) and (b) respectively depict the evolution of position p [m] and velocity v [m/s] for each vehicle. After 45s, the velocity of each vehicle converges to the desired one. Moreover, position errors $\tilde{p}$ [m] and velocity errors $\tilde{v}$ [m/s] of each vehicle are depicted in Fig. 4 (c) and (d), and distance errors between each vehicle are lower than 0.6m. Therefore, by exploiting distributed controller (3), vehicle platoon (1) without a fault is stable.

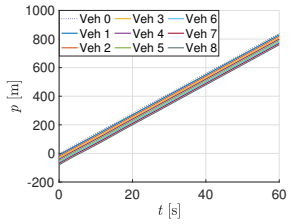

(a) Curves of position of each vehicle.

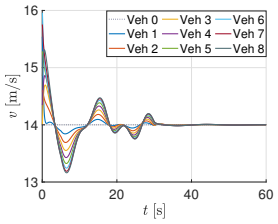

(b) Evolution of velocity of each vehicle.

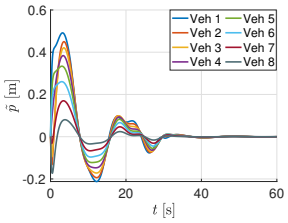

(c) Curves of position errors between the leader and followers.

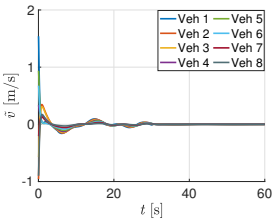

(d) Evolution of velocity errors between the leader and followers.

Fig. 4. Experiment results of the fault-free vehicle platoon.

Case II: A faulty vehicle platoon

TABLE II
Alarm Time for Each Vehicle.

FVs	FTs	ATs	Thresholds
1	0s	0s	0.3865
2	5s	5.32s	0.0975
3	18s	20.16s	0.2219
4	18s	20.22s	0.1851
5	5s	5.68s	0.1271
6	0s	0s	0.2370
7	0s	0s	0.2384
8	0s	0s	0.2121

In this case, take $h = 0.1$s as the sampling period and identical parameters as Case I are applied to solve the following

optimization problem

$$\min \zeta$$
$$s.t.\ (16).$$

Then, we can get the following parameters:

$$\zeta = 0.2434,$$
$$A_f = \begin{pmatrix} -0.0151 & -13.7988 & -147.2638 & -5.4877 \\ -1.0010 & -21.4811 & -83.9246 & -7.6742 \\ -0.0000 & -4.2474 & -28.4630 & -1.3823 \\ 0.0002 & -0.0182 & 0.4435 & -0.0834 \end{pmatrix},$$
$$B_f = \begin{pmatrix} -0.3257 & -0.0417 & 0.0038 \\ -0.0446 & -0.0050 & 0.0012 \\ 0.0017 & 0.0001 & -0.0001 \\ -0.0029 & -0.0003 & -0.0001 \end{pmatrix},$$
$$C_f = \begin{pmatrix} 0.0226 & 0.0293 & -0.2147 & -0.2394 \end{pmatrix},$$
$$D_f = \begin{pmatrix} 0.4949 \\ 0.0613 \\ 0.0106 \end{pmatrix}^T, \kappa = \begin{pmatrix} 0.7369 & 0.0907 & 0.0008 \\ 0.0907 & 0.0121 & 0.0010 \\ 0.0008 & 0.0010 & 0.0010 \end{pmatrix}.$$

In addition, we set fault signal $f_i(t),\ i = 2, \cdots, 5$ as:

$$f_{i\in\{2,5\}}(t) = \begin{cases} \begin{pmatrix} \mathcal{N}(0,5), \mathcal{N}(0,5) \end{pmatrix}^T, & t \in [5\text{s}, 10\text{s}), \\ 0, & \text{otherwise}, \end{cases}$$
$$f_3(t) = \begin{cases} \begin{pmatrix} 4, 3 \end{pmatrix}^T, & t \in [18\text{s}, 22\text{s}), \\ 0, & \text{otherwise}, \end{cases}$$
$$f_4(t) = \begin{cases} \begin{pmatrix} 3, 2 \end{pmatrix}^T, & t \in [18\text{s}, 22\text{s}), \\ 0, & \text{otherwise}, \end{cases}$$

Moreover, the curves of position p [m] and velocity v [m/s] for each faulty vehicle are shown in Fig. 5 (a) and (b). Then, the position errors $\tilde{p}$ [m] and velocity errors $\tilde{v}$ [m/s] are exhibited in Fig. 5 (c) and (d), and it is easily observed that each vehicle keeps a safe distance and the distance errors of each vehicle are lower than 2.5m. Furthermore, in Fig. 6 (a) and Fig. 6 (b), it is easily seen that the change curves of the different residual evaluation function $J_i(t),\ i = 1, 2, \cdots, 8$ for each following vehicle. In addition, the alarm times (ATs) of the following vehicles (FVs), the fault times (FTs) of FVs, and thresholds $J_{th,i},\ i = 1, 2, \cdots, 8$ are also provided in Table II. Moreover, Fig. 6 (c) respectively depicts the evolutions of residual response $r_{e,i}(t), i = 1, 2, \cdots, 8$ for each vehicle without and with a fault, and the evolutions of the PETS with triggered instants and triggered intervals are exhibited in Fig. 6 (d). Consequently, we conclude that the devised fault detection filter can effectively detect the fault for each vehicle.

Case III: A comparison of three different sampling strategies in fault detection filter

In this case, we also apply a periodic sampling (PS) and an ETS to the fault detection filter for the FVs comparison to highlight the performance of the presented PETS, where we use the fixed transmission rate of 50Hz as transmission instants.

The number of triggers (NOTs), average triggering period (ATP), signal update period (SUP), a ratio between the quantity of data transmission in two event-triggered strategies and the quantity of data transmission in periodic sampling, and the

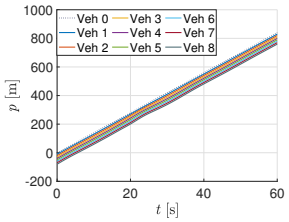

(a) Curves of position of each vehicle.

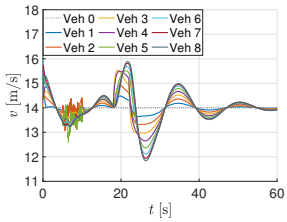

(b) Evolution of velocity of each vehicle.

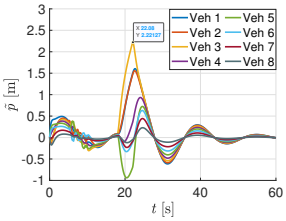

(c) Curves of position errors between the leader and followers.

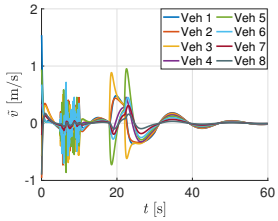

(d) Evolution of velocity errors between the leader and followers.

Fig. 5. Experiment results of the faulty vehicle platoon.

TABLE III
FAULT DETECTION FILTER WITH PS FOR EACH VEHICLE.

FVs	NOTs	SUP	Ratio
1	3000	20ms	100%
2	3000	20ms	100%
3	3000	20ms	100%
4	3000	20ms	100%
5	3000	20ms	100%
6	3000	20ms	100%
7	3000	20ms	100%
8	3000	20ms	100%

TABLE IV
FAULT DETECTION FILTER WITH ETS FOR EACH VEHICLE.

FVs	NOTs	SUP	Ratio
1	311	0.19s	10.37%
2	344	0.17s	11.47%
3	309	0.19s	10.03%
4	306	0.20s	10.02%
5	313	0.19s	10.43%
6	311	0.19s	10.37%
7	311	0.19s	10.37%
8	327	0.18s	10.90%

fault detection filter with the PS, the ETS, and the PETS for the following vehicles (FVs) with undirected communication topology within 60s are respectively shown in Tables III, IV, and V. Based on the three tables, we can see that the NOTs of the ETS and the PS are higher than the PETS and the ATP of ETS and PS are smaller than PETS for each vehicle. Compared with the ETS and the PS, the proposed PETS can effectively reduce 6.24% and 95.74% bandwidth occupation of the network and save more communication resources.

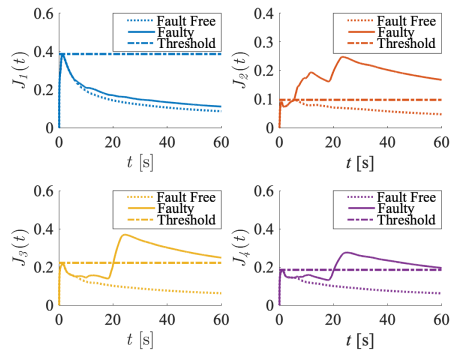

(a) Time evolutions of residual evaluation function $J_i(t), i = 1, 2, 3, 4$.

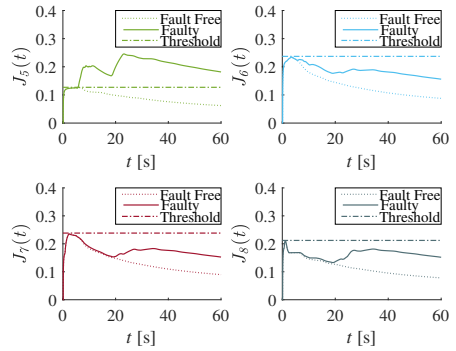

(b) Time evolutions of residual evaluation function $J_i(t), i = 5, 6, 7, 8$.

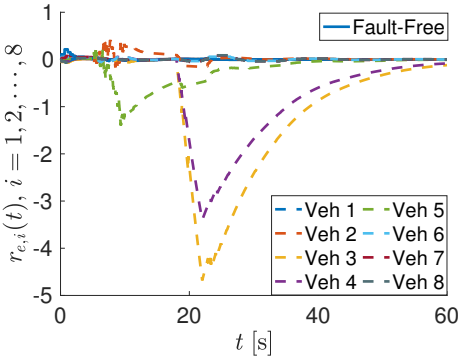

(c) Time evolutions of residual response $r_{e,i}(t), i = 1, 2, \cdots, 8$.

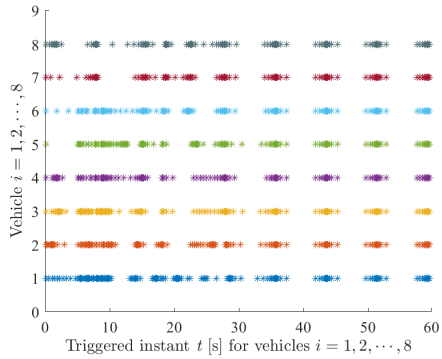

(d) Time evolutions of PETS with sample period $h = 0.1s$ and $\delta_i = 0.2,\ i = 1, 2, \cdots, 8$.

Fig. 6. Experiment results of fault detection and PETS for the vehicle platoon.

TABLE V
FAULT DETECTION FILTER WITH PETS FOR EACH VEHICLE.

FVs	NOTs	SUP	Ratio
1	144	$0.42s$	4.80%
2	142	$0.42s$	4.73%
3	133	$0.45s$	4.43%
4	132	$0.45s$	4.40%
5	116	$0.52s$	3.87%
6	129	$0.46s$	4.30%
7	116	$0.52s$	3.87%
8	110	$0.55s$	3.67%

Fig. 7. Two vehicles used in field experiment validation.

B. Field Experiments

To demonstrate the performance of the designed PETS-based fault detection filter and its technical feasibility in practical application, the theoretical results of this paper are applied to a platoon of 2 test vehicles (see Fig. 7). These vehicles communicate with each other through WiFi under the undirected topology (see Fig. 2), where the initial position, velocity, and acceleration of the leading vehicle are $p_0(0) = 0\text{m}, v_0(0) = 0.8\text{m/s}, a_0(0) = 0\text{m/s}^2$, and these above parameters of 2 following vehicles are respectively defined as $p_1(0) = -3\text{m}, v_1(0) = 0\text{m/s}, a_1(0) = 0\text{m/s}^2, p_2(0) = -6\text{m}, v_2(0) = 0\text{m/s}$, and $a_2(0) = 0\text{m/s}^2$.

Case I: A fault-free vehicle platoon

Considering that there only exist 2 test vehicles (see Fig. 7), we preset and store the predefined state and time-varying trajectory of the leading vehicle in the following vehicle 1 before the experiment begins. For this field experiment, we initially select distributed control gains $k_p = 5.5, k_v = 10, k_a = 1.5$ according to string stability condition (see [46]) and then fine-tune them to obtain satisfactory performance. Next, we choose 3m as a desired following distance, together with several same parameters as Case I of Subsection A. Due to unknown, uncertain, and time-varied external disturbances caused by roads with up and down slopes and wind gusts in the field, clear values of them are not provided. Fig. 8 (a) and (b) show the evolutions of position p [m] and velocity v [m/s] of each real vehicle. Then, the change curves of position errors $\tilde{p}$ [m] and velocity errors $\tilde{v}$ [m/s] are exhibited in Fig. 8 (c) and (d),

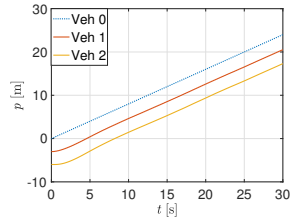

(a) Time evolutions of position of each vehicle.

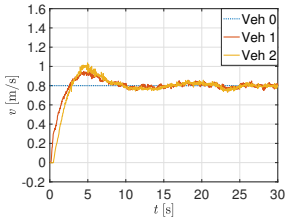

(b) Time evolutions of velocity of each vehicle.

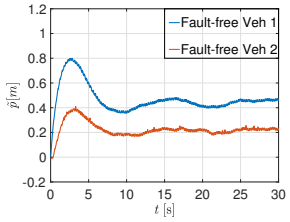

(c) Time evolutions of position errors of fault-free vehicle platoon.

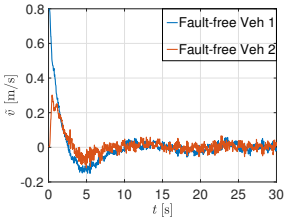

(d) Time evolutions of velocity errors of fault-free vehicle platoon.

Fig. 8. Experiment results of the fault-free vehicle platoon.

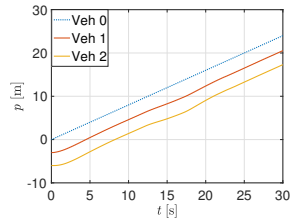

(a) Time evolutions of position of each vehicle.

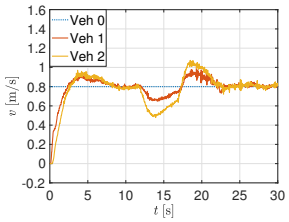

(b) Time evolutions of velocity of each vehicle.

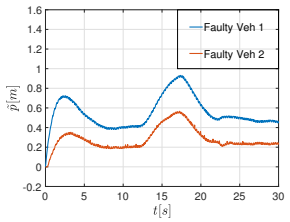

(c) Time evolutions of position errors of faulty vehicle platoon.

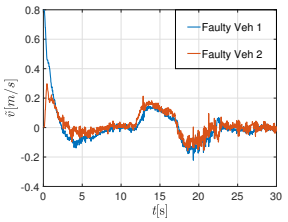

(d) Time evolutions of velocity errors of faulty vehicle platoon.

Fig. 9. Experiment results of the faulty vehicle platoon.

and we can easily observe that $\tilde{p}_1$ [m] approaches to 0.41m and $\tilde{p}_2$ [m] approaches to 0.21m after 30s, which may be caused by external disturbances, but $\tilde{v}$ [m/s] of the following vehicles approach to 0 after 30s.

Case II: A faulty vehicle platoon

We select the same parameters as Subsection A and Case I of this Subsection to solve the following optimization problem:

$$\min \zeta$$
$$s.t.\ (16).$$

Then, we can obtain the following parameters:

$$\zeta = 0.2554,$$

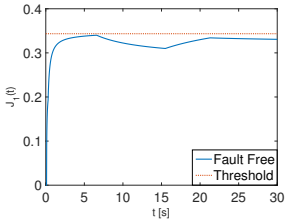

(a) Time evolutions of residual evaluation function $J_1(t)$.

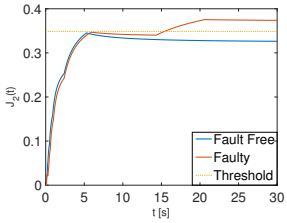

(b) Time evolutions of residual evaluation function $J_2(t)$.

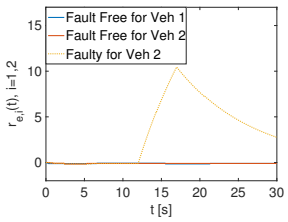

(c) Time evolutions of residual response $r_{e,i}(t), i = 1, 2$.

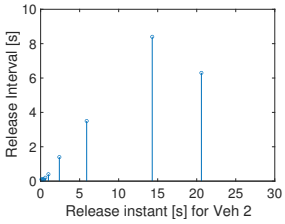

(d) Time evolutions of periodic event-triggered times with sample period $h = 0.1s$ and $\delta_2 = 0.2$.

Fig. 10. Experiment results of fault detection and PETS for the vehicle platoon.

$$A_f = \begin{pmatrix} -0.0165 & -1.7902 & -44.3573 & -0.7497 \\ -1.0005 & -7.4832 & -13.6685 & -2.5247 \\ 0.0001 & -1.9723 & -14.4149 & -0.5123 \\ 0.0003 & -0.0233 & 0.1354 & -0.0927 \end{pmatrix},$$

$$B_f = \begin{pmatrix} -0.2055 & -0.0267 & -0.0017 \\ -0.0373 & -0.0046 & -0.0005 \\ -0.0020 & -0.0004 & -0.0002 \\ -0.0036 & -0.0002 & -0.0000 \end{pmatrix},$$

$$C_f = \begin{pmatrix} 0.0295 & -0.0169 & -0.0389 & -0.2938 \end{pmatrix}^T,$$

$$D_f = \begin{pmatrix} 0.4933 \\ 0.0296 \\ -0.0034 \end{pmatrix}^T, \kappa = \begin{pmatrix} 0.5285 & 0.0483 & 0.0005 \\ 0.0483 & 0.0056 & 0.0009 \\ 0.0005 & 0.0009 & 0.0010 \end{pmatrix}.$$

Moreover, the values of faults in 2 following vehicles are denoted as

$$f_1(t) = 0, f_2(t) = (-2.8\sin(2), -7\sin(2))^T,\ t \in [12\text{s}, 17\text{s}).$$

Fig. 9 (a) and (b) depict the change curves of position p [m] and velocity v [m/s], and it is easy to observe that v_2 decreases during $t \in [12\text{s}, 17\text{s})$, and v_1 also decreases due to the influence of the fault of following vehicle 2. Then, the change curves of position errors $\tilde{p}$ [m] and velocity errors $\tilde{v}$ [m/s] are exhibited in Fig. 9 (c) and (d), and we can easily observe that $\tilde{p}_1$ approaches to 0.41m and $\tilde{p}_2$ approaches to 0.21m after 30s, which may be caused by external disturbances, but $\tilde{v}$ [m/s] of the following vehicles approach to 0 after 30s. Furthermore, Fig. 10 (a) and (b) show the change curves of the different residual evaluation function $J_i(t),\ i = 1, 2$, and it can be easily seen that the actuator fault of following vehicle 2 can be detected by the designed fault detection filter after 15s. Fig. 10 (c) exhibits the evolutions of residual response $r_{e,i}(t), i = 1, 2$ for each following vehicle without and with a fault. In addition, the evolutions of the PETS with triggered instants and triggered intervals are exhibited in Fig. 10 (d). Therefore, we conclude that the devised PETS-based fault

detection filter can effectively detect the fault for a real vehicle platooning system.

Remark 4. Practically, no matter MATLAB simulation or real vehicle experiment, research on fault detection for the vehicle platoon is totally different from the case of a single vehicle due to the influences of faults from neighbor vehicles. Moreover, it may also generate false alarms caused by other vehicles with lower thresholds. Therefore, based on the experiment results, it is not enough to design a local fault detection filter and a passive distributed fault-tolerant controller to deal with the fault problem for each vehicle but ignore the influences of faults from other neighbor vehicles, especially under unknown and random faults. In view of this, it becomes increasingly meaningful and deserves future study to devise an observed-based active fault-tolerant control strategy to estimate and compensate for faults of each vehicle to address influences of faults from neighbor vehicles and ensure safety and string stability for a vehicle platoon.

VI. CONCLUSION

In this paper, we have dealt with a PETS-based fault detection problem for a vehicle platoon subject to external disturbances and actuator faults in the network environment. By designing a PETS-based fault detection filter, not only the actuator faults in the vehicle platoon have been detected in a short time, but also more communication resources are saved. Furthermore, some theorems for guaranteeing stability with H_∞ performance of the residual system have also been formulated based on the Lyapunov-Krasovskii functional and inequality techniques. At last, we have presented the numerical experiments to verify the obtained results.

APPENDIX A
THE PROOF THEOREM 1

Formulate the Lyapunov-Krasovskii functional for system (11) as follows:

$$V(t) = V_1(t) + V_2(t) + V_3(t) + V_4(t), \tag{17}$$

where

$$\begin{aligned}
V_1(t) &= \mathcal{S}^T(t)P\mathcal{S}(t),\\
V_2(t) &= \sum_{i=1}^{N}\left(\int_{t-\tau_m^i}^{t}\mathcal{S}_i^T(\alpha)\tilde{Q}_1\mathcal{S}_i(\alpha)d\alpha\right.\\
&\quad\left.+\int_{t-\tau_M^i}^{t-\tau_m^i}\mathcal{S}_i^T(\alpha)\tilde{Q}_2\mathcal{S}_i(\alpha)d\alpha\right),\\
V_3(t) &= \sum_{i=1}^{N}\left(\tau_m^i\int_{-\tau_m^i}^{0}\int_{t+\alpha}^{t}\dot{\mathcal{S}}_i^T(\beta)\tilde{R}_1\dot{\mathcal{S}}_i(\beta)d\beta d\alpha\right.\\
&\quad\left.+d^i\int_{-\tau_M^i}^{-\tau_m^i}\int_{t+\alpha}^{t}\dot{\mathcal{S}}_i^T(\beta)\tilde{R}_2\dot{\mathcal{S}}_i(\beta)d\beta d\alpha\right),\\
V_4(t) &= \sum_{i=1}^{N}\left[(\tau_M^i)^2\int_{\rho_i h}^{t}\dot{\mathcal{S}}_i^T(\alpha)\tilde{E}\dot{\mathcal{S}}_i(\alpha)d\alpha-\frac{\pi^2}{4}\int_{\rho_i h}^{t}(\mathcal{S}_i(\alpha)\right.\\
&\quad\left.-\mathcal{S}_i(\rho_i h))^T\tilde{E}(\mathcal{S}_i(\alpha)-\mathcal{S}_i(\rho_i h))d\alpha\right].
\end{aligned}$$

Based on Lemma 2, we can easily prove that Lyapunov functional $V_4(t) > 0$.

In what follows, one yields

$$\begin{aligned}
\dot{V}(t) = {} & 2\mathcal{S}^T(t)P\dot{\mathcal{S}}(t)+\sum_{i=1}^{N}\Big(\mathcal{S}_i^T(t)\tilde{Q}_1\mathcal{S}_i(t)-\mathcal{S}_i^T(t-\tau_m^i)\\
&\times\tilde{Q}_1\mathcal{S}_i(t-\tau_m^i)+\mathcal{S}_i^T(t-\tau_m^i)\tilde{Q}_2\mathcal{S}_i(t-\tau_m^i)\\
&-\mathcal{S}_i^T(t-\tau_M^i)\tilde{Q}_2\mathcal{S}_i(t-\tau_M^i)+\dot{\mathcal{S}}_i^T(t)\Big[(\tau_m^i)^2\tilde{R}_1\\
&+d_i^2\tilde{R}_2\Big]\dot{\mathcal{S}}_i(t)-\tau_m^i\int_{t-\tau_m^i}^{t}\dot{\mathcal{S}}_i^T(\alpha)\tilde{R}_1\dot{\mathcal{S}}_i(\alpha)d\alpha\\
&-d^i\int_{t-\tau_M^i}^{t-\tau_m^i}\dot{\mathcal{S}}_i^T(\alpha)\tilde{R}_2\dot{\mathcal{S}}_i(\alpha)d\alpha+(\tau_M^i)^2\dot{\mathcal{S}}_i^T(t)\tilde{E}\dot{\mathcal{S}}_i(t)\\
&-\frac{\pi^2}{4}[\mathcal{S}_i(t)-\mathcal{S}_i(t-\tau_i(t))]^T\tilde{E}[\mathcal{S}_i(t)-\mathcal{S}_i(t-\tau_i(t))]\Big).
\end{aligned}\tag{18}$$

Based on Lemma 1, we acquire

$$-\tau_m^i\int_{t-\tau_m^i}^{t}\dot{\mathcal{S}}_i^T(\alpha)\tilde{R}_1\dot{\mathcal{S}}_i(\alpha)d\alpha\leqslant\mathcal{S}_{1,i}^T(t)\hat{\tilde{R}}_1\mathcal{S}_{1,i}(t),\tag{19}$$

where $\hat{\tilde{R}}_1=\begin{pmatrix}-\tilde{R}_1 & \tilde{R}_1\\ * & -\tilde{R}_1\end{pmatrix}$, $\mathcal{S}_{1,i}(t)=(\mathcal{S}_i^T(t),\mathcal{S}_i^T(t-\tau_m^i))^T$.

According to Lemma 3, for a matrix $\tilde{G}$ fulfilling $\begin{pmatrix}\tilde{R}_2 & \tilde{G}\\ * & \tilde{R}_2\end{pmatrix}>0$, one obtains

$$-d^i\int_{t-\tau_M^i}^{t-\tau_m^i}\dot{\mathcal{S}}_i^T(\alpha)\tilde{R}_2\dot{\mathcal{S}}_i(\alpha)d\alpha\leqslant\mathcal{S}_{2,i}^T(t)\hat{\tilde{R}}_2\mathcal{S}_{2,i}(t),\tag{20}$$

where $\hat{\tilde{R}}_2=\begin{pmatrix}-\tilde{R}_2 & \tilde{R}_2-\tilde{G} & \tilde{G}\\ * & [\tilde{G}-\tilde{R}_2]_s & \tilde{R}_2-\tilde{G}\\ * & * & -\tilde{R}_2\end{pmatrix}$, $\mathcal{S}_{2,i}(t)=(\mathcal{S}_i^T(t-\tau_m^i),\mathcal{S}_i^T(t-\tau_i(t)),\mathcal{S}_i^T(t-\tau_M^i))^T$.

Substituting (19) and (20) into (18), one has

$$\begin{aligned}
\dot{V}(t)\leqslant{} & 2\mathcal{S}^T(t)P(\Phi_1\mathcal{S}(t)+\Phi_2\mathcal{S}(t-\tau(t))+\Phi_3\vartheta(t)+\Phi_4\mathbf{e}(t))\\
&+\mathcal{S}^T(t)(I_N\otimes\tilde{Q}_1)\mathcal{S}(t)-\mathcal{S}^T(t-\tau_m)(I_N\otimes\tilde{Q}_1)\\
&\times\mathcal{S}(t-\tau_m)+\mathcal{S}^T(t-\tau_m)(I_N\otimes\tilde{Q}_2)\mathcal{S}(t-\tau_m)\\
&-\mathcal{S}^T(t-\tau_M)(I_N\otimes\tilde{Q}_2)\mathcal{S}(t-\tau_M)\\
&+\dot{\mathcal{S}}^T(t)\left(\tau_m^2\otimes\tilde{R}_1+d^2\otimes\tilde{R}_2+\tau_M^2\otimes\tilde{E}\right)\dot{\mathcal{S}}(t)\\
&+\mathcal{S}_1^T(t)\bar{R}_1\mathcal{S}_1(t)+\mathcal{S}_2^T(t)\bar{R}_2\mathcal{S}_2(t)-\frac{\pi^2}{4}[\mathcal{S}(t)\\
&-\mathcal{S}(t-\tau(t))]^T(I_N\otimes\tilde{E})[\mathcal{S}(t)-\mathcal{S}(t-\tau(t))],
\end{aligned}$$

where $\mathcal{S}(t-\tau_m)=(\mathcal{S}_1^T(t-\tau_m^1),\mathcal{S}_2^T(t-\tau_m^2),\cdots,\mathcal{S}_N^T(t-\tau_m^N))^T$, $\mathcal{S}(t-\tau_M)=(\mathcal{S}_1^T(t-\tau_M^1),\mathcal{S}_2^T(t-\tau_M^2),\cdots,\mathcal{S}_N^T(t-\tau_M^N))^T$, $\mathcal{S}_1(t)=(\mathcal{S}^T(t),\mathcal{S}^T(t-\tau_m))^T$, $\mathcal{S}_2(t)=(\mathcal{S}^T(t-\tau_m),\mathcal{S}^T(t-\tau(t)),\mathcal{S}^T(t-\tau_M))^T$,

$$\bar{R}_1=\begin{pmatrix}-I_N\otimes\tilde{R}_1 & I_N\otimes\tilde{R}_1\\ * & -I_N\otimes\tilde{R}_1\end{pmatrix},$$

$$\bar{R}_2=\begin{pmatrix}-I_N\otimes\tilde{R}_2 & I_N\otimes(\tilde{R}_2-\tilde{G}) & I_N\otimes\tilde{G}\\ * & I_N\otimes([\tilde{G}-\tilde{R}_2]_s) & I_N\otimes(\tilde{R}_2-\tilde{G})\\ * & * & -I_N\otimes\tilde{R}_2\end{pmatrix}.$$

Then, we need to prove that residual system (11) fulfills asymptotically stability in respect of $\vartheta(t)=0$.

From (6), it is clear that for $t \in [t_k^i h + \eta_k^i, t_{k+1}^i h + \eta_{k+1}^i)$

$$\begin{aligned} e_i^T(t)\kappa e_i(t) &\leqslant \delta_i \tilde{y}_i^T(t-\tau_i(t))\kappa \tilde{y}_i(t-\tau_i(t)) \\ &= \delta_i \tilde{z}_i^T(t-\tau_i(t))C^T\kappa C\tilde{z}_i(t-\tau_i(t)). \end{aligned}$$

Denote $\mathcal{S}_3(t) = (\mathcal{S}^T(t), \mathcal{S}^T(t-\tau_m), \mathcal{S}^T(t-\tau(t)), \mathcal{S}^T(t-\tau_M), \mathbf{e}^T(t))^T$. In what follows, we can yield

$$\dot{V}(t) \leqslant \mathcal{S}_3^T(t)\Psi_2\mathcal{S}_3(t),$$

where $\Psi_2 = \Psi_3 + \check{\Phi}_1^T(\tau_m^2 \otimes R_1^{-1})\check{\Phi}_1 + \check{\Phi}_2^T(d^2 \otimes R_2^{-1})\check{\Phi}_2 + \check{\Phi}_3^T(\tau_M^2 \otimes E^{-1})\check{\Phi}_3, \check{\Phi}_1 = \check{\Phi}^T(I_N \otimes (\epsilon^T R_1)), \check{\Phi}_2 = \check{\Phi}^T(I_N \otimes (\epsilon^T R_2)), \check{\Phi}_3 = \check{\Phi}^T(I_N \otimes (\epsilon^T E)), \check{\Phi} = (\Phi_1, 0_{8N\times 8N}, \Phi_2, 0_{8N\times 8N}, \Phi_4)$,

$$\Psi_3 = \begin{pmatrix} \chi_{11} & I_N \otimes \tilde{R}_1 & \chi_{13} & \tilde{0} & \chi_{16} \\ * & \chi_{22} & \chi_{23} & I_N \otimes \tilde{G} & \bar{0} \\ * & * & \chi_{33} & \chi_{23} & \bar{0} \\ * & * & * & \chi_{44} & \bar{0} \\ * & * & * & * & -I_N \otimes \kappa \end{pmatrix}.$$

According to Schur complement, it can be obtained that $\Psi_2 < 0$ can be ensured by (14). Then, we can also prove $\dot{V}(t) < 0$. Consequently, residual system (11) fulfills asymptotic stability.

Next, according to the definition of H_∞ performance (12) of residual system (11), one acquires:

$$\mathcal{H}(t) = \int_0^t \left(\mathbf{r}_e^T(\omega)\mathbf{r}_e(\omega) - \zeta^2\vartheta^T(\omega)\vartheta(\omega)\right)d\omega,$$

Then, one gets

$$\begin{aligned} &\int_0^t \left(\mathbf{r}_e^T(\omega)\mathbf{r}_e(\omega) - \zeta^2\vartheta^T(\omega)\vartheta(\omega)\right)d\omega \\ \leqslant &\int_0^t \Big(\mathbf{r}_e^T(\omega)\mathbf{r}_e(\omega) - \zeta^2\vartheta^T(\omega)\vartheta(\omega) + \dot{V}(\omega) + \tilde{y}^T(\omega-\tau(\omega)) \\ &\times(\delta\otimes\kappa)\tilde{y}(\omega-\tau(\omega)) - e^T(\omega)(I_N\otimes\kappa)e(\omega)\Big)d\omega. \\ \leqslant &\int_0^t \mathcal{S}_4^T(\omega)\Psi_5\mathcal{S}_4(\omega)d\omega, \end{aligned}$$

where $\tilde{y}(\omega-\tau(\omega)) = (\tilde{y}_1^T(\omega-\tau_1(\omega)), \tilde{y}_2^T(\omega-\tau_2(\omega)), \cdots, \tilde{y}_N^T(\omega-\tau_N(\omega)))^T, \mathcal{S}_4(t) = (\mathcal{S}^T(t), \mathcal{S}^T(t-\tau_m), \mathcal{S}^T(t-\tau(t)), \mathcal{S}^T(t-\tau_M), \vartheta^T(t), \mathbf{e}^T(t))^T, \Psi_5 = \Psi_4 + \tilde{\Phi}_1^T(\tau_m^2 \otimes R_1^{-1})\tilde{\Phi}_1 + \tilde{\Phi}_2^T(d^2\otimes R_2^{-1})\tilde{\Phi}_2 + \tilde{\Phi}_3^T(\tau_M^2\otimes E^{-1})\tilde{\Phi}_3 + \tilde{\Phi}_1^T\tilde{\Phi}_1$.

Based on Schur complement and the condition of (14), we can easily get $\mathcal{H}(t) < 0$, which ensures system (11) to satisfy H_∞ performance (12). □

APPENDIX B
THE PROOF THEOREM 2

Define matrices $P = \begin{pmatrix} I_N\otimes\hat{P}_1 & I_N\otimes\hat{P}_2 \\ * & I_N\otimes\hat{P}_3 \end{pmatrix}$ and $\Gamma = (I_N\otimes(\hat{P}_2\hat{P}_3^{-1}))$. Then, by using elementary transformation and congruence transformation diag$[I_{4N}, \Gamma, I_{4N}, I_{4N}, I_{4N}, I_{2N}, I_{3N}, I_{4N}, I_{4N}, I_{4N}, I_N]$ to (14), condition (15) can be easily acquired, and some new variables are defined: $\hat{A}_f = \hat{P}_2A_f\hat{P}_3^{-1}\hat{P}_2^T, \hat{B}_f = \hat{P}_2B_f, \hat{C}_f = C_f\hat{P}_3^{-1}, \hat{D}_f = D_f$.

Then, according to the proof of Theorem 1, we conclude that (15) can ensure residual system (11) fulfilling asymptotic stability with H_∞ performance (12). □

APPENDIX C
THE PROOF THEOREM 3

For (15), matrix $\mathcal{L}+\mathcal{M}$ is symmetric and other matrices are block diagonal matrices. Define an orthogonal matrix $\mathcal{X} \in \mathbb{R}^{N\times N}$ fulfilling $\mathcal{X}^{-1} = \mathcal{X}^T$ such that $\mathcal{X}^{-1}(\mathcal{L}+\mathcal{M})\mathcal{X} = \varsigma$ with $\varsigma = \text{diag}\,[\varsigma_1, \varsigma_2, \cdots, \varsigma_N]$ and $\varsigma_i = \lambda_i(\mathcal{L}+\mathcal{M})$. Let $\tilde{\mathcal{X}}^{-1} = \text{diag}\,[\tilde{\mathcal{X}}^{-1}, I_{5N}, I_{4N}, I_{4N}, I_{4N}, I_{2N}, I_{3N}, I_{4N}, I_{4N}, I_{4N}, I_N]$, where $\tilde{\mathcal{X}}^{-1} = \mathcal{X}^{-1}\otimes I_3$. In what follows, one has

$$\hat{\Psi}_2 = \hat{\mathcal{X}}^{-1}\hat{\Psi}_1\hat{\mathcal{X}},$$

where

$$\begin{aligned} \hat{\Psi}_2 &= \begin{pmatrix} \hat{\Psi}_5 & \hat{\check{\Phi}}_1 & \hat{\check{\Phi}}_2 & \hat{\check{\Phi}}_3 & \bar{\check{\Phi}}_2^T \\ * & -\hat{\tilde{R}}_1 & \tilde{0} & \tilde{0} & \check{0} \\ * & * & -\hat{\tilde{R}}_2 & \tilde{0} & \check{0} \\ * & * & * & -\hat{\tilde{E}} & \check{0} \\ * & * & * & * & -I_N \end{pmatrix}, \\ \hat{\Psi}_5 &= \begin{pmatrix} \hat{\tilde{\chi}}_{11} & \hat{R}_1 & \hat{\chi}_{13} & \hat{\tilde{0}} & \hat{\chi}_{15} & \hat{\chi}_{16} \\ * & \hat{\chi}_{22} & \hat{\chi}_{23} & I_N\otimes G & \hat{\tilde{0}} & \hat{\tilde{0}} \\ * & * & \hat{\chi}_{33} & \hat{\chi}_{23} & \hat{\tilde{0}} & \hat{\tilde{0}} \\ * & * & * & \hat{\chi}_{44} & \hat{\tilde{0}} & \hat{\tilde{0}} \\ * & * & * & * & \chi_{55} & \hat{0} \\ * & * & * & * & * & -\hat{\kappa} \end{pmatrix}, \\ \hat{\tilde{\chi}}_{11} &= \begin{pmatrix} \bar{\tilde{\chi}}_{11} & \bar{A}_f + \bar{\tilde{A}}^T\Gamma \\ * & \bar{A}_f + \bar{A}_f^T \end{pmatrix}, \\ \hat{\tilde{\Phi}}_1 &= \hat{\tilde{\Phi}}^T(I_N\otimes R_1), \hat{\tilde{\Phi}}_2 = \hat{\tilde{\Phi}}^T(I_N\otimes R_2), \\ \bar{\tilde{\chi}}_{11} &= I_N\otimes(Q_1 - R_1 - \frac{\pi^2}{4}E) + [(I_N\otimes\hat{P}_1)\bar{\tilde{A}}]_s, \\ \bar{\tilde{A}} &= \text{diag}[I_N\otimes A - \varsigma\otimes BK, I_N\otimes A_w], \\ \hat{\tilde{\Phi}}_3 &= \hat{\tilde{\Phi}}^T(I_N\otimes E), \hat{\tilde{\Phi}} = (\bar{\tilde{A}}, 0_{4N\times 16N}, \hat{\Phi}_3, 0_{4N\times 3N}). \end{aligned}$$

Considering that $\mathcal{X}$ is an orthogonal matrix fulfilling $\mathcal{X}^{-1} = \mathcal{X}^T$, then we can get $\hat{\Psi}_1 < 0 \Leftrightarrow \hat{\Psi}_2 < 0$.

Moreover, the submatrices in $\hat{\Psi}_2 < 0$ are in a decomposable form and are block diagonal, then $\hat{\Psi}_2$ can be decomposed into a small condition for all ς_i as follows, such that $\hat{\Psi}_2 < 0$ when and only when condition (16) holds. Thus, we complete the proof of Theorem 3. □

REFERENCES

[1] H. Yao, X. Li, and X. Yang, "Physics-aware learning-based vehicle trajectory prediction of congested traffic in a connected vehicle environment," *IEEE Transactions on Vehicular Technology*, vol. 72, no. 1, pp. 102-112, 2023.

[2] H. X. Liu, X. Wu, W. Ma, and H. Hu, "Real-time queue length estimation for congested signalized intersections," *Transportation Research Part C: Emerging Technologies*, vol. 17, no. 4, pp. 412-427, 2009.

[3] M. Hu, C. Li, Y. Bian, H. Zhang, Z. Qin, and B. Xu, "Fuel economy-oriented vehicle platoon control using economic model predictive control," *IEEE Transactions on Intelligent Transportation Systems*, vol. 23, no. 11, pp. 20836-20849, 2022.

[4] C. Chen, J. Wang, Q. Xu, J. Wang, and K. Li, "Mixed platoon control of automated and human-driven vehicles at a signalized intersection: dynamical analysis and optimal control," *Transportation Research Part C: Emerging Technologies*, vol. 127, pp. 103138, 2021.

[5] S. E. Shladover, "Opportunities and challenges in cooperative road vehicle automation," *IEEE Open Journal of Intelligent Transportation Systems*, vol. 2, pp. 216-224, 2021.

[6] C. N. Mokogwu and K. Hashtrudi-Zaad, "Energy-based analysis of string stability in vehicle platoons," *IEEE Transactions on Vehicular Technology*, vol. 71, no. 6, pp. 5915-5929, 2022.

[7] S. Feng, Y. Zheng, S. E. Li, Z. Cao, and H. X. Liu "String stability for vehicular platoon control: Definitions and analysis methods," *Annual Reviews in Control*, vol. 47, pp. 81-97, 2019.

[8] Y. Zheng, Y. Bian, S. Li, and S. E. Li, "Cooperative control of heterogeneous connected vehicles with directed acyclic interactions," *IEEE Intelligent Transportation Systems Magazine*, vol. 13, no. 2, pp. 127-141, Summer 2021.

[9] J. I. Ge and G. Orosz, "Optimal control of connected vehicle systems with communication delay and driver reaction time," *IEEE Transactions on Intelligent Transportation Systems*, vol. 18, no. 8, pp. 2056-2070, 2017.

[10] S. B. Prathiba, G. Raja, K. Dev, N. Kumar, and M. Guizani, "A hybrid deep reinforcement learning for autonomous vehicles smart-platooning," *IEEE Transactions on Vehicular Technology*, vol. 70, no. 12, pp. 13340-13350, 2021.

[11] R. Valiente, B. Toghi, R. Pedarsani, and Y. P. Fallah, "Robustness and adaptability of reinforcement learning-based cooperative autonomous driving in mixed-autonomy traffic," *IEEE Open Journal of Intelligent Transportation Systems*, vol. 3, pp. 397-410, 2022.

[12] W. Bai, X. Yao, H. Dong, and X. Lin, "Mixed $H\_/H_\infty$ fault detection filter design for the dynamics of high speed train," *Science China Information Sciences*, vol. 60, pp. 048201, 2017.

[13] S. Salih and R. Olawoyin, "Fault injection in model-based system failure analysis of highly automated vehicles," *IEEE Open Journal of Intelligent Transportation Systems*, vol. 2, pp. 417-428, 2021.

[14] M. Gao, L. Sheng, D. Zhou, and Y. Niu, "Event-based fault detection for T-S fuzzy systems with packet dropouts and (x, v)-dependent noises," *Signal Processing*, vol. 138, pp. 211-219, 2017.

[15] Wang S, Zhao D, Yuan J, Li H, Gao Y. "Application of NSGA-II algorithm for fault diagnosis in power system," *Electric Power Systems Research*, vol. 175, pp. 105893, 2019.

[16] X. He, Z. Wang, and D. H. Zhou, "Robust fault detection for networked systems with communication delay and data missing," *Automatica*, vol. 45, no. 11, pp. 2634-2639, 2009.

[17] X. J. Li and G. H. Yang "Dynamic observer-based robust control and fault detection for linear systems," *IET Control Theory and Applications*, vol. 6, no. 17, pp. 2657-2666, 2012.

[18] G. -H. Yang, H. Wang, and L. Xie, "Fault detection for output feedback control systems with actuator stuck faults: A steady-state-based approach. *International Journal of Robust and Nonlinear Control*, vol. 20, no. 15, pp. 1739-1757, 2010.

[19] X. Wang, Z. Fei, H. Yan, and Y. Xu, "Dynamic event-triggered fault detection via zonotopic residual evaluation and its application to vehicle lateral dynamics," *IEEE Transactions on Industrial Informatics*, vol. 16, no. 11, pp. 6952-6961, 2020.

[20] J. Wang, F. Ma, Y. Yang, J. Nie, B. Aksun-Guvenc, and L. Guvenc, "Adaptive event-triggered platoon control under unreliable communication links," *IEEE Transactions on Intelligent Transportation Systems*, vol. 23, no. 3, pp. 1924-1935, 2022.

[21] S. Öncü, J. Ploeg, N. van de Wouw, and H. Nijmeijer, "Cooperative adaptive cruise control: network-aware analysis of string stability," *IEEE Transactions on Intelligent Transportation Systems*, vol. 15, no. 4, pp. 1527-1537, 2014.

[22] F. Gao, X. Hu, S. E. Li, K. Li, and Q. Sun, "Distributed adaptive sliding mode control of vehicle platoon with uncertain interaction topology," *IEEE Transaction on Industrial Electronics*, vol. 65, no. 8, pp. 6352-6361, 2018.

[23] N. T. Hung, A. M. Pascoal, and T. A. Johansen, "Cooperative path following of constrained autonomous vehicles with model predictive control and event-triggered communications," *International Journal of Robust and Nonlinear Control*, vol. 30, no. 7, pp. 2644-2670, 2020.

[24] X. Wang and M. D. Lemmon, "Event-triggering in distributed networked control systems," *IEEE Transactions on Automatic Control*, vol. 56, no. 3, pp. 586-601, 2011.

[25] C. Peng and T. Yang, "Event-triggered communication and H_∞ control co-design for networked control systems," *Automatica*, vol. 49, no. 5, pp. 1326-1332, 2011.

[26] W. Ren and D. V. Dimarogonas, "Event-triggered tracking control of networked multi-agent systems," *IEEE Transactions on Automatic Control*, vol. 67, no. 10, pp. 5332-5347, 2022.

[27] G. D. Khan, Z. Chen, and L. Zhu, "A new approach for event-triggered stabilization and output regulation of nonlinear systems," *IEEE Transactions on Automatic Control*, vol. 65, no. 8, pp. 3592-3599, 2020.

[28] G. Wu, G. Chen, H. Zhang, and C. Huang, "Fully distributed event-triggered vehicle platooning with actuator uncertainties," *IEEE Transactions on Vehicular Technology*, vol. 70, no. 7, pp. 6601-6612, 2021.

[29] X. Ge, S. Xiao, Q. -L. Han, X. -M. Zhang, and D. Ding, "Dynamic event-triggered scheduling and platooning control co-design for automated vehicles over vehicle ad-hoc networks," *IEEE/CAA Journal of Automatica Sinica*, vol. 9, no. 1, pp. 31-46, 2022.

[30] W. P. M. H. Heemels, M. C. F. Donkers, and A. R. Teel, "Periodic event-triggered control for linear systems," *IEEE Transactions on Automatic Control*, vol. 58, no. 4, pp. 847-861, 2013.

[31] W. Wang, R. Postoyan, D. Nešić, and W. P. M. H. Heemels, "Periodic event-triggered control for nonlinear networked control systems," *IEEE Transactions on Automatic Control*, vol. 65, no. 2, pp. 620-635, 2020.

[32] S. Wen, G. Guo, B. Chen, and X. Gao, "Event-triggered cooperative control of vehicle platoons in vehicular ad hoc networks," *Information Sciences*, vol. 459, pp. 341-353, 2018.

[33] K. Halder, U. Montanaro, S. Dixit, M. Dianati, A. Mouzakitis, and S. Fallah, "Distributed H_∞ controller design and robustness analysis for vehicle platooning under random packet drop," *IEEE Transactions on Intelligent Transportation Systems*, vol. 23, no. 5, pp. 4373-4386, 2022.

[34] Y. Zheng, S. E. Li, K. Li, and W. Ren, "Platooning of connected vehicles with undirected topologies: Robustness analysis and distributed H-infinity controller synthesis," *IEEE Transactions on Intelligent Transportation Systems*, vol. 19, no. 5, pp. 1353-1364, 2018.

[35] J. Hu, P. Bhowmick, F. Arvin, A. Lanzon, and B. Lennox, "Cooperative control of heterogeneous connected vehicle platoons: An adaptive leader-following approach," *IEEE Robotics and Automation Letters*, vol. 5, no. 2, pp. 977-984, April 2020.

[36] Y. Bian, Y. Zheng, W. Ren, S. E. Li, J. Wang, and K. Li, "Reducing time headway for platooning of connected vehicles via V2V communication," *Transportation Research Part C*, vol. 102, pp. 87-105, 2019.

[37] G. Guo and W. Yue, "Autonomous platoon control allowing range-limited sensors," *IEEE Transactions on Vehicular Technology*, vol. 61, no. 7, pp. 2901-2912, 2012.

[38] F. Gao, S. E. Li, Y. Zheng, and D. Kum, "Robust control of heterogeneous vehicle platoon with uncertain dynamics and communication delay," *IET Intelligent Transport Systems*, vol. 10, no. 7, pp. 503-513, 2012.

[39] S. Dong, Z. -G. Wu, P. Shi, H. R. Karimi, and H. Su, "Networked fault detection for Markov jump nonlinear systems," *IEEE Transactions on Fuzzy Systems*, vol. 26, no. 6, pp. 3368-3378, 2018.

[40] P. M. Frank and X. Ding, "Survey of robust residual generation and evaluation methods in observer-based fault detection systems," *Journal of Process Control*, vol. 7, no. 6, pp. 403-424, 1997.

[41] K. Gu, "An integral inequality in the stability problem of time-delay systems," *Proceedings of the 39th IEEE Conference on Decision and Control*, vol. 3, pp. 2805-2820, 2000.

[42] K. Liu and E. Fridman, "Wirtinger's inequality and Lyapunov-based sampled-data stabilization," *Automatica*, vol. 48, no. 1, pp. 102-108, 2012.

[43] X. Wang, Z. Fei, H. Gao, and J. Yu, "Integral-based event-triggered fault detection filter design for unmanned surface vehicles," *IEEE Transactions on Industrial Informatics*, vol. 15, no. 10, pp. 5626-5636, 2019.

[44] J. Dai and G. Guo "Event-triggered leader-following consensus for multi-agent systems with semi-Markov switching topologies," *Information Sciences*, vol. 459, pp. 290-301, 2018.

[45] L. Ding and G. Guo, "Distributed event-triggered H_∞ consensus filtering in sensor networks," *Signal Processing*, vol. 108, pp. 365-375, 2015.

[46] Y. Zheng, S. Eben Li, J. Wang, D. Cao, and K. Li, "Stability and scalability of homogeneous vehicle platoon: study on the influence of information flow topologies," *IEEE Transactions on Intelligent Transportation Systems*, vol. 17, no. 1, pp. 14-26, 2016.

Lu Wang received the B.E. and M. E. degrees from Tiangong University, Tianjin, China, in 2018 and 2021. She is currently pursuing a Ph.D. degree at the College of Mechanical and Vehicle Engineering, Hunan University, Changsha, China. Her current research interests include adaptive control, fault-tolerant control, fault detection, distributed control, and their applications to connected and automated vehicles.

Manjiang Hu received the B.Tech. and Ph.D. degrees from Jiangsu University, China, in 2009 and 2014, respectively. He has worked as a Post-Doctoral Researcher at the Department of Automotive Engineering, Tsinghua University, from 2014 to 2017. He is currently a Professor with the College of Mechanical and Vehicle Engineering and the State Key Laboratory of Advanced Design and Manufacturing Technology for Vehicle, Hunan University, Changsha, China. His research interests include cooperative driving assistance technology and vehicle control, etc.

Yougang Bian (Member, IEEE) received the B.E. and Ph.D. degrees from Tsinghua University, Beijing, China, in 2014 and 2019, respectively. He was a Visiting Scholar with the Department of Electrical and Computer Engineering, University of California at Riverside, from 2017 to 2018. He is currently an Associate Professor with the College of Mechanical and Vehicle Engineering and the State Key Laboratory of Advanced Design and Manufacturing Technology for Vehicle, Hunan University, Changsha, China. His research interests include distributed control, cooperative control, and their applications to connected and automated vehicles. He was a recipient of the Best Paper Award at the *2017 IEEE Intelligent Vehicles Symposium*.

Ge Guo (Senior Member, IEEE) received the B.S. and Ph.D. degrees from Northeastern University, Shenyang, China, in 1994 and 1998, respectively. From May 2000 to April 2005, he was with the Lanzhou University of Technology, China, as a Professor and the Director with the Institute of Intelligent Control and Robots. He then joined Dalian Maritime University, Dalian, China, as a Professor. Since 2018, he has been a Professor with Northeastern University and the Dean with the School of Control Engineering, Qinhuangdao Campus. He has authored or coauthored more than 150 international journal papers in his research interests which include intelligent transportation systems and cyber-physical systems. Dr. Guo is currently an Associate Editor for the IEEE TRANSACTIONS ON INTELLIGENT TRANSPORTATION SYSTEMS, IEEE TRANSACTIONS ON INTELLIGENT VEHICLES, *Information Sciences, IEEE Intelligent Transportation Systems Magazine, ACTA Automatica Sinica, China Journal of Highway and Transport, and the Journal of Control and Decision.* He was the recipient of an honoree of the New Century Excellent Talents in University, Ministry of Education, China, in 2004, and nominee for Gansu Top Ten Excellent Youths by the Gansu Provincial Government in 2005, CAA Young Scientist Award in 2017, and the First Prize of Natural Science Award of Hebei Province in 2020.

Shengbo Eben Li (Senior Member, IEEE) received the M.S. and Ph.D. degrees from Tsinghua University in 2006 and 2009. He worked at Stanford University, University of Michigan, and University of California, Berkeley. He is currently a tenured professor at Tsinghua University. His active research interests include intelligent vehicles and driver assistance, reinforcement learning and distributed control, optimal control and estimation, etc. He was the recipient of Best Paper Award in 2014 IEEE ITS Symposium, National Award for Technological Invention in China (2013), Excellent Young Scholar of NSF China (2016), Young Professorship of Changjiang Scholar Program (2016). He is now the IEEE senior member and serves as associated editor of IEEE ITSM and IEEE Trans. ITS, etc.

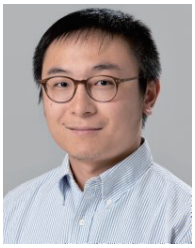

Boli Chen (Member, IEEE) received the B.Eng. degree in electrical and electronic engineering from Northumbria University, Newcastle upon Tyne, U.K., in 2010, and the M.Sc. and Ph.D. degrees in control systems from Imperial College London, London, U.K., in 2011 and 2015, respectively. He is currently a Lecturer with the Department of Electronic and Electrical Engineering, University College London, London, U.K. His research interests include control, optimization, estimation and identification of a range of complex dynamical systems, mainly from automotive, and power electronics areas.

Zhihua Zhong received the Ph.D. degree in engineering from Linköping University, Sweden, in 1988. He is currently a Professor with the School of Vehicle and Mobility, Tsinghua University. He is an Elected Member of the Chinese Academy of Engineering. His research interests include auto collision security technology, the punching and shaping technologies of the auto body, modularity and lightweighing auto technologies, and vehicle dynamics.